Ensuring Advancement in Sandwich Construction Through Innovation and Exploitation

REPORT

No.: D3.3 – part 5

Introduction of loads into axially loaded sandwich panels

Publisher:	Saskia Käpplein Thomas Misiek Karlsruher Institut für Technologie (KIT) Versuchsanstalt für Stahl, Holz und Steine

Task:	3.4
Object:	Design of axially loaded sandwich panels - load application areas

This report includes 54 pages.

Date of issue: 10.10.2011

Versuchsanstalt für Stahl, Holz und Steine, Karlsruher Institut für Technologie (KIT) Tel.: +49 (0)721 608 42215
Abt. Stahl- und Leichtmetallbau, D-76128 Karlsruhe, Deutschland Fax: +49 (0)721 608 44078

This report may only be reproduced in an unabridged version. A publication in extracts needs our written approval.

Project co-funded under the European Commission Seventh Research and Technology Development Framework Programme (2007-2013) Theme 4 NMP-Nanotechnologies, Materials and new Production Technologies		
Prepared by		
Saskia Käpplein, Thomas Misiek, Karlsruher Institut für Technologie (KIT), Versuchsanstalt für Stahl, Holz und Steine		
Drafting History		
Draft Version 1.1	06.10.2011	
Draft Version 1.2		
Draft Version 1.3		
Draft Version 1.4		
Final	10.10.2011	
Dissemination Level		
PU	Public	X
PP	Restricted to the other programme participants (including the Commission Services)	
RE	Restricted to a group specified by the Consortium (including the Commission Services)	
CO	Confidential, only for members of the Consortium (including the Commission Services)	
Verification and approval		
Coordinator		
Industrial Project Leader		
Management Committee		
Industrial Committee		
Deliverable		
D3.3 – part 5: Introduction of loads into axially loaded sandwich panels	Due date: Month 35 Completed: Month 37	

This report may only be reproduced in an unabridged version. A publication in extracts needs our written approval.

Table of contents

This report may only be reproduced in an unabridged version. A publication in extracts needs our written approval.

Symbols and notations

A_F	cross section area of face
E_F	elastic modulus of face
E_C	elastic modulus of core
G_C	shear modulus of core
I_F	moment of inertia of a face
EI_F	bending stiffness of a face
N_{cr}	elastic buckling load
c	stiffness of elastic foundation
t_F	thickness of face
$f_{y,F}$	yield strength of face
α	imperfection factor (equivalent member method)
λ_w	slenderness of face (wrinkling in mid-span)
λ_c	slenderness of face (crippling of free edge)
ν_C	Poisson ratio of core material
ν_F	Poisson ratio of face sheet
$\sigma_{cr,w}$	elastic buckling stress (wrinkling in mid-span)
$\sigma_{cr,c}$	elastic buckling stress (crippling of free edge)
σ_w	wrinkling stress
σ_c	crippling stress
χ_w	reduction factor for wrinkling (equivalent member method)
χ_c	reduction factor for crippling (equivalent member method)

This report may only be reproduced in an unabridged version. A publication in extracts needs our written approval.

1 Introduction

Until now the common application of sandwich panels is restricted to the function of space enclosure. The sandwich panels are mounted on a substructure and they transfer transverse loads as wind and snow to the substructure. The sandwich panels are subjected to bending moments and transverse forces only. A new application is to apply sandwich panels with flat or lightly profiled faces in smaller buildings – such as cooling chambers, climatic chambers and clean rooms – without any load transferring substructure (Fig. 1.1).

Fig. 1.1: Building made of sandwich panels but without substructure

In this new type of application in addition to space enclosure, the sandwich panels have to transfer loads and to stabilise the building. In addition to the moments and transverse forces resulting from transverse loads, the wall panels transfer normal forces arising from the superimposed load from overlying roof or ceiling panels. Within the framework of work package 3 of the EASIE project, design methods for axially loaded sandwich panels have been developed. In Deliverable D3.3 – part 4 [1] design procedures for global design are introduced.

The report at hand deals with the design of the areas of load application, i.e. with the lower end of the panel and at the connection between wall and roof, where the superimposed loads from the roof are applied as normal force into the wall panel. Load application details, at which the normal force is introduced by contact, are considered in the report.

Tests on load application details were performed. The tests are documented in test report D3.2 – part 5 [2]. Based on these tests and on numerical calculations a procedure for the design of the load application area is derived. With this procedure the load bearing capacity of the load application area can be determined based on the wrinkling stress of the compressed face.

This report may only be reproduced in an unabridged version. A publication in extracts needs our written approval.

2 Load application details

The report at hand deals with load application areas, e.g. the connection between wall and roof. Two examples of load application details are shown in Fig. 2.1. At the load application area the axial force is introduced from the roof into the wall or from the wall into the foundation by contact.

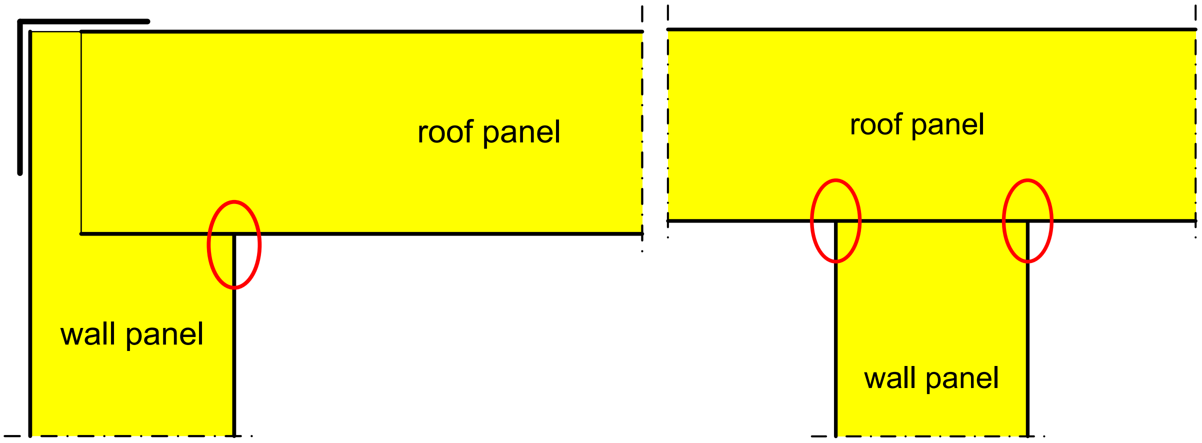

Fig. 2.1: Examples of load application details

Amongst other things ETAG 21 [8] deals also with the design of axially loaded panels. A test procedure for determination of the resistance to axial loads is given in Annex D of ETAG 21. In these tests the assembly of a wall panel and its fixings is tested. The panel is fixed to the foundation as in practice. Also the load is introduced as in the intended application.

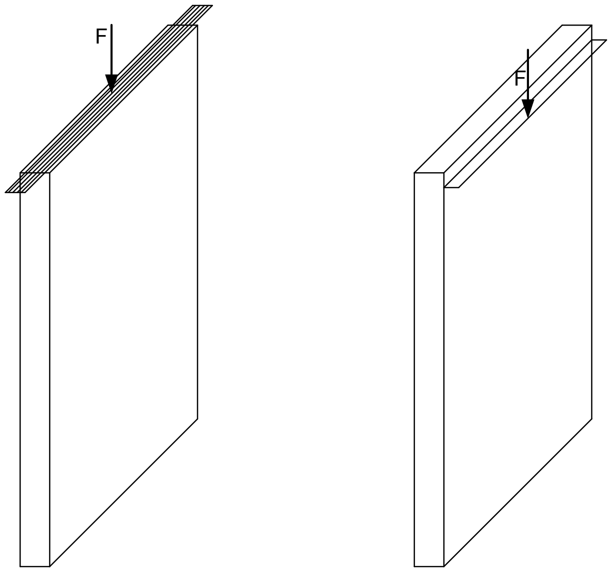

Fig. 2.2: Test according to ETAG 21 for centric and eccentric axial load

So by tests according to ETAG 21 the resistance to axial loads is determined for the tested configuration of panel and fixing only. There are only few possibilities to use a resistance

This report may only be reproduced in an unabridged version. A publication in extracts needs our written approval.

value, which is determined by these tests, for any other configuration. Furthermore ETAG 21 makes no distinction between the global load-bearing capacity of the panel and the local load bearing capacity of the load application area. No general resistance values, which can be used for a generalized design method, are determined, by the procedures according to ETAG 21.

3 Tests on load application details

3.1 Tested specimens

Different tests on load application details, where the loads are introduced as a normal force into the face of a panel, were performed. For all tests specimens with the width 400 mm have been used. The tested specimens had the length of approximately 300 mm – 400 mm. Panels with steel faces and different core materials have been tested. A summary of the tested types of panels is given in the following table.

No.	core material	thickness of panel [mm]	face material	thickness of faces [mm]	profiling of faces
A	PU	100	steel	0,50	lightly profiled
B *)	PU	100	steel	0,75	lightly profiled
C	EPS	100	steel	0,60	flat
E	MW	100	steel	0,50	lightly profiled
*) discontinuous produced panel					

Tab. 3.1: Tested types of sandwich panels

For each tested type of panel the mechanical properties of the face sheets and of the core material were determined. In addition bending tests to determine the wrinkling stress of the faces have been performed.

From the face sheets specimens for tensile tests according to EN 10002-1 were worked out and tensile tests for determining the mechanical properties of surface layers were done. For the determination of the yield strength $R_{eH}/R_{p0,2}$ and the tensile strength R_m the core thicknesses t_k determined on the specimens were used. The mean values of the results are listed in Tab. 3.2.

This report may only be reproduced in an unabridged version. A publication in extracts needs our written approval.

type of panel		t_K [mm]	$R_{eH}/R_{p0,2}$ [N/mm²]	R_m [N/mm²]
A	top side of production	0,474	358	405
	bottom side of production	0,472	358	403
B	top side of production	0,765	399	403
	bottom side of production	0,759	406	402
C	face 1	0,538	412	456
	face 2	0,541	406	453
E	face 1	0,474	461	468
	face 2	0,476	472	479

Tab. 3.2: Mechanical properties of the faces (mean values)

The mechanical properties of the core layer were determined according to EN 14509 [3]. The determination of the compression strength f_{Cc}, the tensile strength f_{Ct}, the shear strength f_{Cv}, as well as the appropriate shear, compression and tensile module values G_C, E_{Cc} and E_{Ct} was realized on at least three specimens. The analysis of the modulus of elasticity E_C was realised as mean value from the compression and tensile module of a specimen pair. The mean values of the results are listed in Tab. 3.3 and Tab. 3.4.

No.	f_{Cv} [N/mm²]	f_{Cc} [N/mm²]	f_{Ct} [N/mm²]
A	0,09	0,10	0,14
B	0,11	0,19	0,21
C	0,10	0,15	0,16
E	0,08	0,09	0,12

Tab. 3.3: Mechanical properties of the core layer – strength (mean values)

No.	G_C [N/mm²]	E_{Cc} [N/mm²]	E_{Ct} [N/mm²]	E_C [N/mm²]
A	2,93	2,95	3,24	3,10
B	3,56	3,83	6,32	5,08
C	4,18	6,38	10,56	8,47
E	9,82	9,33	12,08	10,71

Tab. 3.4: Mechanical properties of the core layer – module (mean values)

To determine the wrinkling stress single-span bending tests were performed with every type of sandwich panel. The sandwich panels with a length of 6000 mm were loaded until failure in a vacuum chamber under uniform surface load. For the calculation of the wrinkling stress the

This report may only be reproduced in an unabridged version. A publication in extracts needs our written approval.

measured core thickness of the steel faces and the measured thickness of the panels were used. The results of the single-span bending tests are listed in Tab. 3.5.

type of panel		thickness of panel (mean value)	width of panel	span	core sheet thickness of com-pressed face	failure load incl. dead weight	wrinkling stress
		[mm]	[mm]	[mm]	[mm]	[kN/m]	[N/mm²]
		D	B	l_a	t_K	p	σ_w
A	top side of production	99,4	1176	5700	0,474	2,69	198
	bottom side of production	99,3	1178	5700	0,472	2,75	203
B	top side of production	98,9	1194	5700	0,765	4,41	200
	bottom side of production	89,9	1195	5700	0,759	4,43	202
C	face 1	100,3	1196	5700	0,538	2,79	174
	face 2	100,2	1196	5700	0,541	2,76	177
E	face 1	99,4	999	5800	0,475	1,17	105
	face 2	99,5	999	5800	0,475	1,51	136
		99,4	1000	5800	0,475	1,69	151

Tab. 3.5: Wrinkling stress of the faces

Furthermore the geometry of the lightly profiled faces was measured and the bending stiffness EI_F and the cross section area A_F of the faces were determined. The measured geometries are given in Fig. 3.1. Tab. 3.6 shows the calculated bending stiffness's and areas.

type of panel	area A_F [mm²/mm]	moment of inertia I_F [mm⁴/mm]	bending stiffness EI_F [Nmm²/mm]
A	0,474	0,0764	17635
B	0,762	0,1267	29242
C	0,540	0,0144	3028
E	0,475	0,0194	4477

Tab. 3.6: Area and bending stiffness of faces

This report may only be reproduced in an unabridged version. A publication in extracts needs our written approval.

Panel type A:

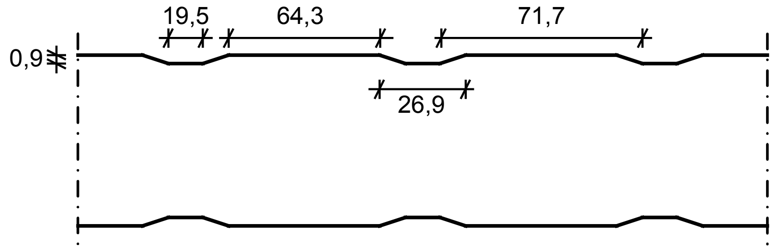

Panel type B:

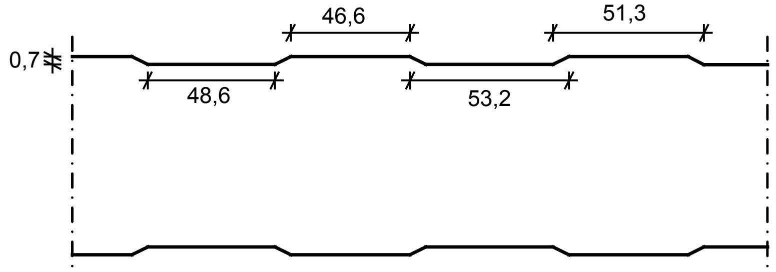

Panel type E:

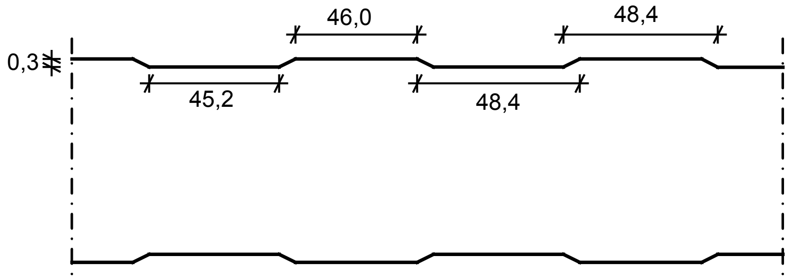

Fig. 3.1: Geometry of the faces

To fix the specimens to the test set-up aluminium angles were glued and additionally screwed to the faces at the lower end of the specimens. The angles were screwed to a wooden board, which could be easily fixed to the test set-up (Fig. 3.2).

Fig. 3.2: Lower end of the tested specimens

This report may only be reproduced in an unabridged version. A publication in extracts needs our written approval.

3.2 Introduction of loads by contact

Tests to determine the load bearing capacity of the free cut edge of the panels were performed. The load was introduced by contact. The test set-up is shown in Fig. 3.3 und Fig. 3.4. For introducing the load into the face of the panel a plate of steel has been used. For comparison instead of a plate of steel a section of a sandwich panel was used for introducing the load in some tests (Fig. 3.5). The kind of load introduction did not have a relevant influence on the load bearing behaviour and capacity.

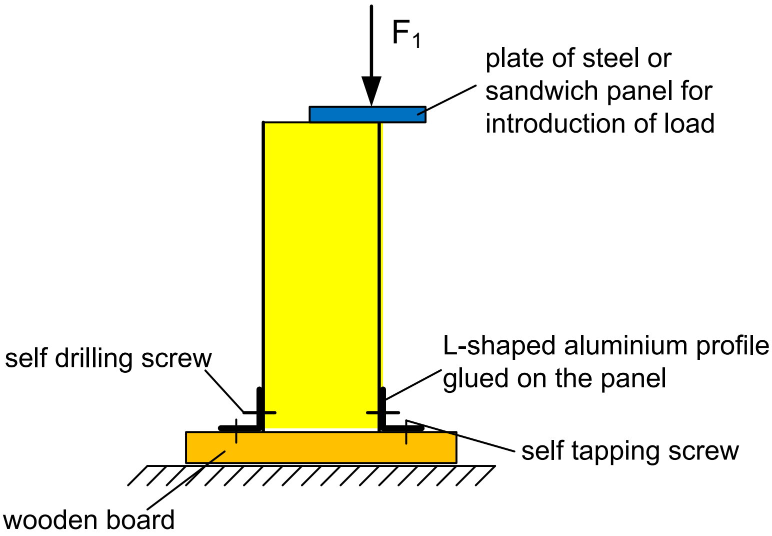

Fig. 3.3: Test set-up

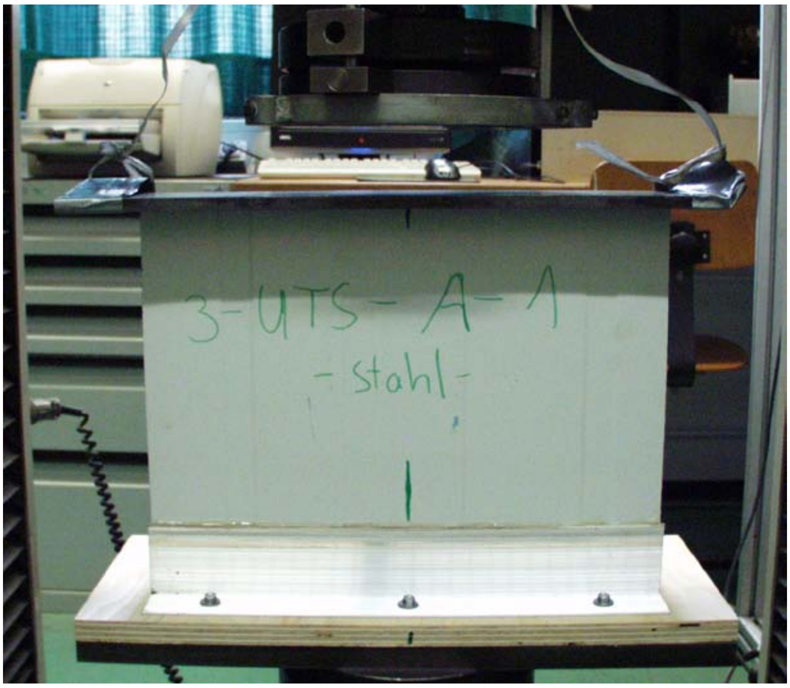

Fig. 3.4: Test set-up

This report may only be reproduced in an unabridged version. A publication in extracts needs our written approval.

Fig. 3.5: Introduction of load by plate of steel and by sandwich panel

In all of the tests a local failure at the load application area occurred. The panels failed by crippling of the face sheet at the loaded free edge.

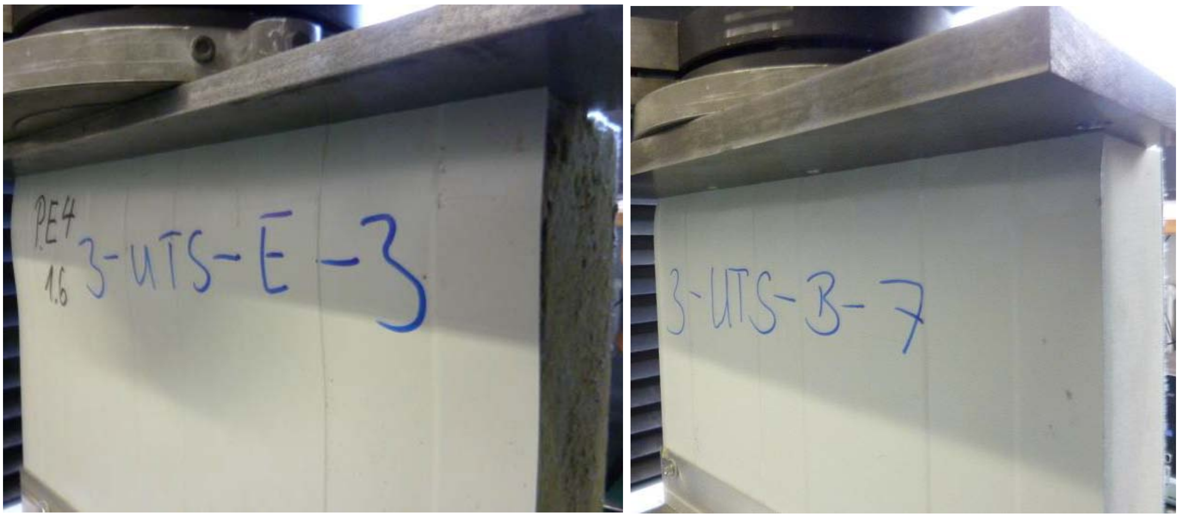

Fig. 3.6: Failure mode crippling of the face sheet

In the tests the ultimate load was determined. In the following tables the results of the tests are summarised. In addition to the ultimate load the ultimate stress in the loaded face sheet is given. The ultimate stress was determined using the measured width of the specimen and the core thickness of the face sheet.

This report may only be reproduced in an unabridged version. A publication in extracts needs our written approval.

type of panel	stressed face	number of test	ultimate load [kN]	ultimate stress [N/mm²]
A	top side of production	1	11,26	59,54
		2*)	13,98	74,48
		3*)	14,03	74,56
	bottom side of production	4**)	12,53	66,53
		5**)	12,11	64,79
		6**)	14,58	78,00
		7**)	12,50	66,71

*) introduction of load by sandwich panel

**) 2 tests performed with one specimen, test of 2nd face

Tab. 3.7: Test results – panel type A

type of panel	stressed face	number of test	ultimate load [kN]	ultimate stress [N/mm²]
B	-	1	19,24	63,12
		2	29,95	98,26
		3	21,42	70,45
		4	29,61	97,39
		5	29,02	95,21
		6	19,40	63,65
		7	19,54	64,27
		8	21,33	70,16
		9	28,01	92,13
		10	20,33	66,87
		11*)	15,30	50,32
		12	16,16	53,15
		13*)	14,82	48,62
		14	20,16	66,14
		15	24,13	79,17
		16	20,60	67,59

*) introduction of load by sandwich panel

Tab. 3.8: Test results – panel type B

This report may only be reproduced in an unabridged version. A publication in extracts needs our written approval.

type of panel	stressed face	number of test	ultimate load [kN]	ultimate stress [N/mm2]
C	-	1	12,26	58,32
		2	9,89	46,93
		3*)	10,02	47,67
		4*)	12,18	57,94
		5	7,18	34,16
		6**)	7,89	37,44
		7**)	8,26	39,29
		8**)	12,26	58,32
*) introduction of load by sandwich panel **) 2 tests performed with one specimen, test of 2nd face				

Tab. 3.9: Test results – panel type C

type of panel	stressed face	number of test	ultimate load [kN]	ultimate stress [N/mm²]
E	-	1	12,14	63,74
		2	12,37	64,94
		4	12,97	68,26
		5	12,32	64,68
		6	9,96	52,29
		7	11,50	60,51
		8	9,13	48,05
		9	8,04	42,32
		10	11,66	61,37
		11	8,71	45,73
		12	11,18	58,70
		13	10,19	53,63
		14	12,36	64,89
		15	9,12	47,88
		16	10,87	57,07
		17	12,76	67,16
		18	10,51	55,32
		19*)	7,93	41,7
		20*)	7,90	41,6
*) introduction of load by sandwich panel				

Tab. 3.10: Test results – panel type E

This report may only be reproduced in an unabridged version. A publication in extracts needs our written approval.

3.3 Tests on corner details

Tests on typical corner details for the connection of wall and roof were performed. The test set up is shown in Fig. 3.7 and Fig. 3.8. To introduce the axial load into the panel a plate of steel was used. An aluminium profile was placed on the plate of steel and on an additional hinged support. The load was introduced into the profile. In addition to the applied load F_1 the reaction force F_2 at the hinged support was measured. The load introduced into the face of the panel can be calculated by subtracting F_2 from F_1.

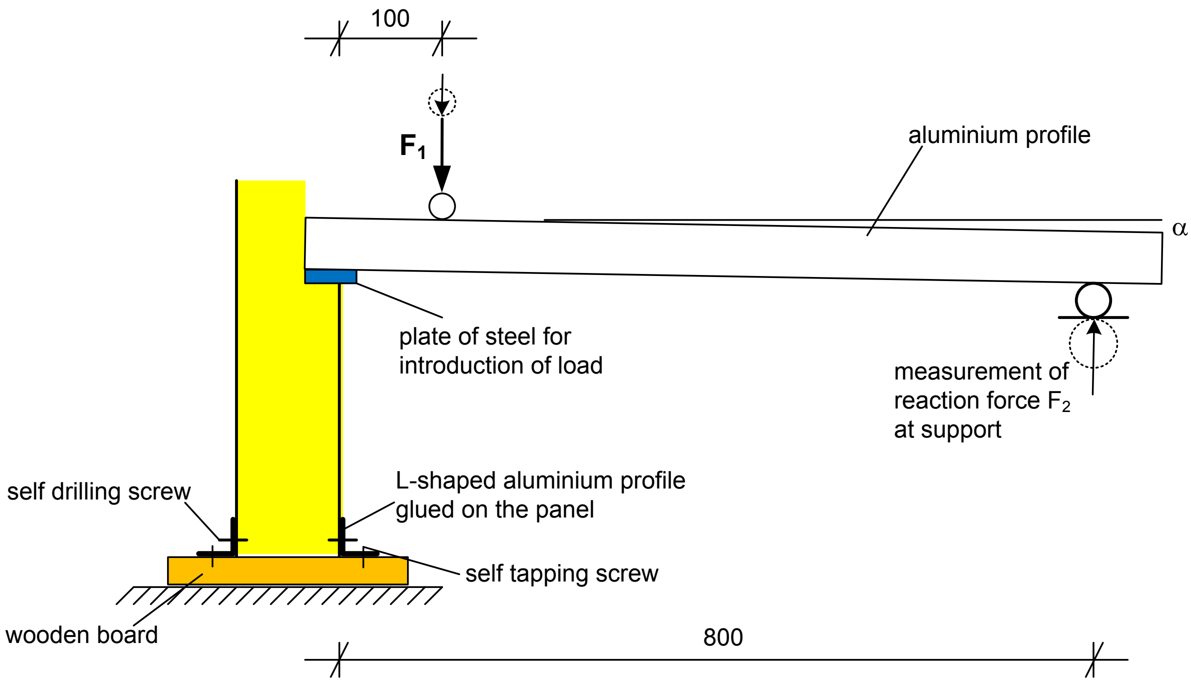

Fig. 3.7: **Test set-up**

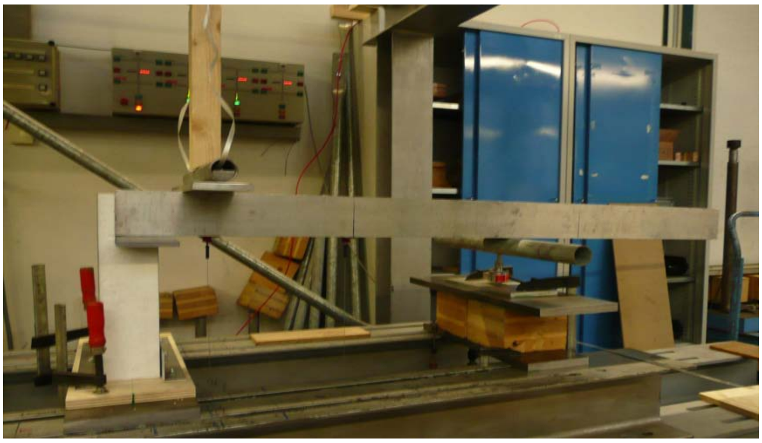

Fig. 3.8: **Test set-up**

In all of the tests a local failure at the load application area occurred. The panels failed by crippling of the face sheet at the loaded free edge.

This report may only be reproduced in an unabridged version. A publication in extracts needs our written approval.

Fig. 3.9: **Failure mode**

In the following tables the results of the tests are summarised. The ultimate loads introduced into the face sheet (F_1 - F_2) and the corresponding ultimate stresses are given.

type of panel	number of test	ultimate load [kN]	ultimate stress [N/mm²]
A	1	16,29	85,9
	2	15,01	79,4
	3	13,93	73,7
	4	13,26	70,1
	5	12,63	66,6
	6	17,27	91,5
	7	16,17	85,5

Tab. 3.11: **Test results – panel type A**

type of panel	number of test	ultimate load [kN]	ultimate stress [N/mm²]
B	1	26,28	86,2
	2	25,72	84,4
	3	25,70	84,3
	4	20,55	67,3
	5	18,43	60,5
	6	19,37	63,6
	7	20,56	67,4
	8	24,67	80,9
	9	23,90	78,4
	10	27,80	91,4
	11	18,86	61,9
	12	19,88	65,2

Tab. 3.12: **Test results – panel type B**

This report may only be reproduced in an unabridged version. A publication in extracts needs our written approval.

type of panel	number of test	ultimate load [kN]	ultimate stress [N/mm²]
C	1	12,05	56,0
	2	7,10	33,7
	3	8,88	42,1
	4	11,20	53,2

Tab. 3.13: Test results – panel type C

type of panel	number of test	ultimate load [kN]	ultimate stress [N/mm²]
E	1	10,93	57,5
	2	9,68	50,9
	3	8,82	46,4
	4	9,02	47,5
	5	10,52	55,4

Tab. 3.14: Test results – panel type E

4 Mechanical basics

4.1 Stability failure modes of a compressed face

The faces of sandwich panels consist of comparatively thin steel sheets. So they have a very high slenderness. If they are subjected to compression forces stability failure may occur. The compressed face sheet fails by a kind of buckling. So the ultimate stress of a face sheet subjected to compression is usually clearly lower than the yield strength of the face material.
At load application area the failure mode of the compressed face is crippling of the free edge. This failure mode is strongly related to wrinkling of a compressed face in mid-span.

Fig. 4.1: Crippling at load application area

This report may only be reproduced in an unabridged version. A publication in extracts needs our written approval.

Fig. 4.2: Wrinkling in mid-span

Crippling as well as wrinkling are stability failure modes. In both cases the face sheet can be regarded as a plate, which is elastically supported by the core material.

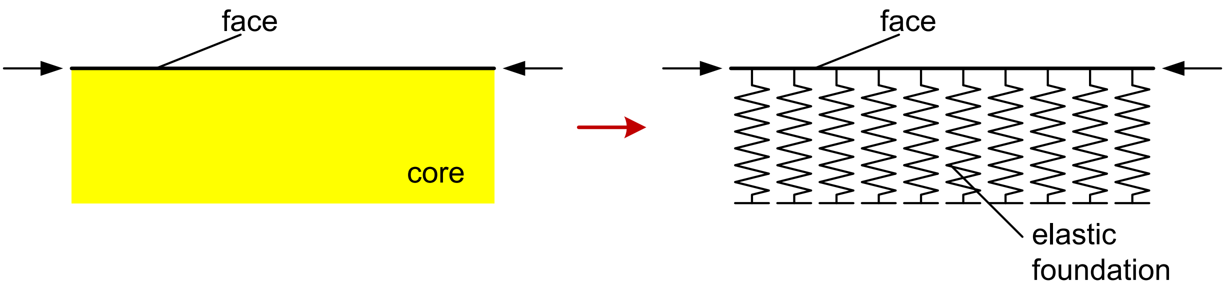

Fig. 4.3: Elastically supported face sheet

4.2 Elastic buckling loads for local buckling of the face

In mid-span we have an infinite plate. So both ends are supported. The elastic buckling stress (wrinkling) of the plate is [15]

$$\sigma_{cr,w} = \frac{3}{2} \cdot \frac{\sqrt[3]{2 \cdot c^2 \cdot EI_F}}{A_F} \cdot \qquad (4.1)$$

The length of the buckling have waves is [15]

$$a_w = \pi \cdot \sqrt[3]{\frac{2 \cdot EI_F}{c}} \qquad (4.2)$$

with

stiffness of elastic foundation:

$$c = \frac{2 \cdot (1 - \nu_C)}{3 - 4 \cdot \nu_C} \cdot \sqrt{\frac{2 \cdot G_C \cdot E_C}{1 + \nu_C}} \qquad (4.3)$$

EI_F bending stiffness of face

This report may only be reproduced in an unabridged version. A publication in extracts needs our written approval.

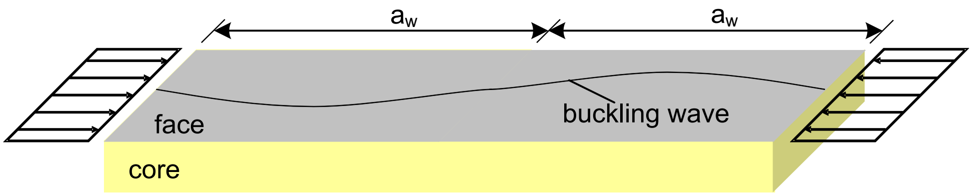

Fig. 4.4: Buckling of a face sheet

Formulae (4.1) and (4.2) were developed for panels with flat faces. The load bearing behaviour of lightly profiled faces is very similar to the behaviour of flat faces. Because of that (4.1) and (4.2) can also be used for lightly profiled faces [15].

If formula (4.3) is rewritten, we get for the stiffness of the elastic foundation

$$c = A \cdot \sqrt{G_C \cdot E_C} \tag{4.4}$$

A is a factor which depends only on the Poisson ratio ν_C of the core material.

$$A = \frac{2 \cdot (1 - \nu_C)}{3 - 4\nu_C} \cdot \sqrt{\frac{2}{1 + \nu_C}} \tag{4.5}$$

In Tab. 4.1 the factor A is given for different Poisson ratio.

ν_C	A
0	0,943
0,1	0,934
0,2	0,939
0,3	0,965
0,4	1,024
0,5	1,155

Tab. 4.1: Relation of Poisson ratio and factor A of formula (4.5)

For core materials as polyurethane or expanded polystyrene the Poisson ratio is between 0,0 and 0,3. For these values the influence of the Poisson ratio on the factor A is very small (approx. 2%). Therefore also the influence on the stiffness c of the elastic foundation and consequently on the length of the buckling waves and on the elastic buckling stress of the face is very small. In the following for the core material a Poisson ratio $\nu_C = 0$ is assumed. With this assumption we get for the stiffness of the elastic foundation

$$c = \frac{2}{3} \cdot \sqrt{2 \cdot G_C \cdot E_C} \tag{4.6}$$

With the stiffness c given above the elastic buckling stress and the length of the buckling half wave are

This report may only be reproduced in an unabridged version. A publication in extracts needs our written approval.

$$\sigma_{cr,w} = \frac{3}{A_F} \cdot \sqrt[3]{\frac{2}{9} \cdot EI_F \cdot G_C \cdot E_C} \qquad (4.7)$$

$$a_w = \pi \cdot \sqrt[6]{\frac{9 \cdot EI_F^2}{2 \cdot G_C \cdot E_C}} \qquad (4.8)$$

For panels with flat face sheets the following formulae can be inserted in (4.7) and (4.8).

$$A_F = t_F \qquad (4.9)$$

$$EI_F = E_F \cdot \frac{t_F^3}{12 \cdot \left(1 - \nu_F^2\right)} \qquad (4.10)$$

With ν_F = 0,3 (steel) for plane faces the elastic buckling stress and the length of the buckling half waves are

$$\sigma_{cr,w} = 3 \cdot \sqrt[3]{\frac{2}{9} \cdot \frac{E_F}{12 \cdot \left(1 - \nu_F^2\right)} \cdot G_C \cdot E_C} = 0{,}82 \cdot \sqrt[3]{E_F \cdot G_C \cdot E_C} \qquad (4.11)$$

$$a_w = \pi \cdot t_F \cdot \sqrt[6]{\frac{9 \cdot E_F^2}{2 \cdot G_C \cdot E_C \cdot \left(12 \cdot \left(1 - \nu_F^2\right)\right)^2}} = 1{,}82 \cdot t_F \cdot \sqrt[6]{\frac{E_F^2}{G_C \cdot E_C}} \qquad (4.12)$$

The slenderness of a compressed component is calculated by the following formulae [6].

$$\lambda = \sqrt{\frac{A \cdot f_y}{N_{cr}}} \qquad (4.13)$$

Based on this the slenderness of the elastically supported infinite face is

$$\lambda_w = \sqrt{\frac{f_{y,F}}{\sigma_{cr,w}}} \qquad (4.14)$$

At the load application area the normal force is introduced into the free edge of the face. So the face corresponds to a semi-infinitely elastically supported plate. Only one end of the plate is supported; the other one is free.

From the theory of beams on elastic foundation the following elastic buckling loads are known [9], [10].

For an infinite beam (both ends supported) the elastic buckling load is

$$N_{cr} = 2 \cdot \sqrt{k \cdot EI} \qquad (4.15)$$

with

k stiffness of elastic foundation

For a semi-infinite beam (free end) the elastic buckling load is half of the load of the infinite beam.

This report may only be reproduced in an unabridged version. A publication in extracts needs our written approval.

$$N_{cr} = \sqrt{k \cdot EI} \tag{4.16}$$

Analogously the elastic buckling stress of a semi-infinite plate on an elastic foundation (crippling of free edge) is

$$\sigma_{cr,c} = \frac{1}{2} \cdot \sigma_{cr,w} \tag{4.17}$$

With the simplification $\nu_C = 0$ introduced above the elastic buckling stress of the free edge is

$$\sigma_{cr,c} = \frac{3}{2 \cdot A_F} \cdot \sqrt[3]{\frac{2}{9} \cdot EI_F \cdot G_C \cdot E_C} \tag{4.18}$$

For plane faces we get the following elastic buckling stress

$$\sigma_{cr,c} = 0{,}41 \cdot \sqrt[3]{E_F \cdot G_C \cdot E_C} \tag{4.19}$$

The slenderness of the semi-infinite plate on an elastic foundation is

$$\lambda_c = \sqrt{\frac{f_{y,F}}{\sigma_{cr,c}}} = \sqrt{\frac{f_{y,F}}{\frac{1}{2}\sigma_{cr,w}}} = \sqrt{2} \cdot \lambda_w \tag{4.20}$$

The buckling length of the semi-infinite plate is (for $\nu_C = 0$)

$$a_c = \sqrt{2} \cdot a_w = \sqrt{2} \cdot \pi \cdot \sqrt[6]{\frac{9 \cdot B_F^2}{2 \cdot G_C \cdot E_C}} \tag{4.21}$$

For plane faces the buckling length can be simplified to

$$a_c = 2{,}574 \cdot t_F \cdot \sqrt[6]{\frac{E_F^2}{G_C \cdot E_C}} \tag{4.22}$$

4.3 Buckling loads for local buckling of the face

If the ultimate load of a compressed component is determined by testing, it usually differs clearly from the elastic buckling load. This is caused by geometrical and material non-linearity as well as by different imperfections, which may influence the load bearing capacity. These effects can be considered by a calculation according to 2nd order theory. In this calculation initial deformations have to be taken into account as imperfections. To cover all imperfections (e.g. initial deformations, material imperfections, residual stresses) an equivalent geometrical imperfection can be used [6]. An initial deformation is considered, which has the same effects as the real imperfections. For the initial deformation the most disadvantageous shape has to be used. This is usually the first eigenmode. To determine the wrinkling or crippling stress of

This report may only be reproduced in an unabridged version. A publication in extracts needs our written approval.

the compressed face of a sandwich panel, as geometrical imperfection an initial deformation of the face is assumed. The initial deformation corresponds to the first eigenmode of wrinkling in mid-span or crippling of the free edge respectively.

Alternatively to a calculation by 2nd order theory a calculation by the equivalent member method with buckling curves can be performed to determine the buckling load of a compressed member [6]. Depending on the slenderness of the component a reduction factor is determined. With the reduction factor the yield strength is reduced to the buckling stress.

$$\sigma_{w/c} = \chi \cdot f_y \tag{4.23}$$

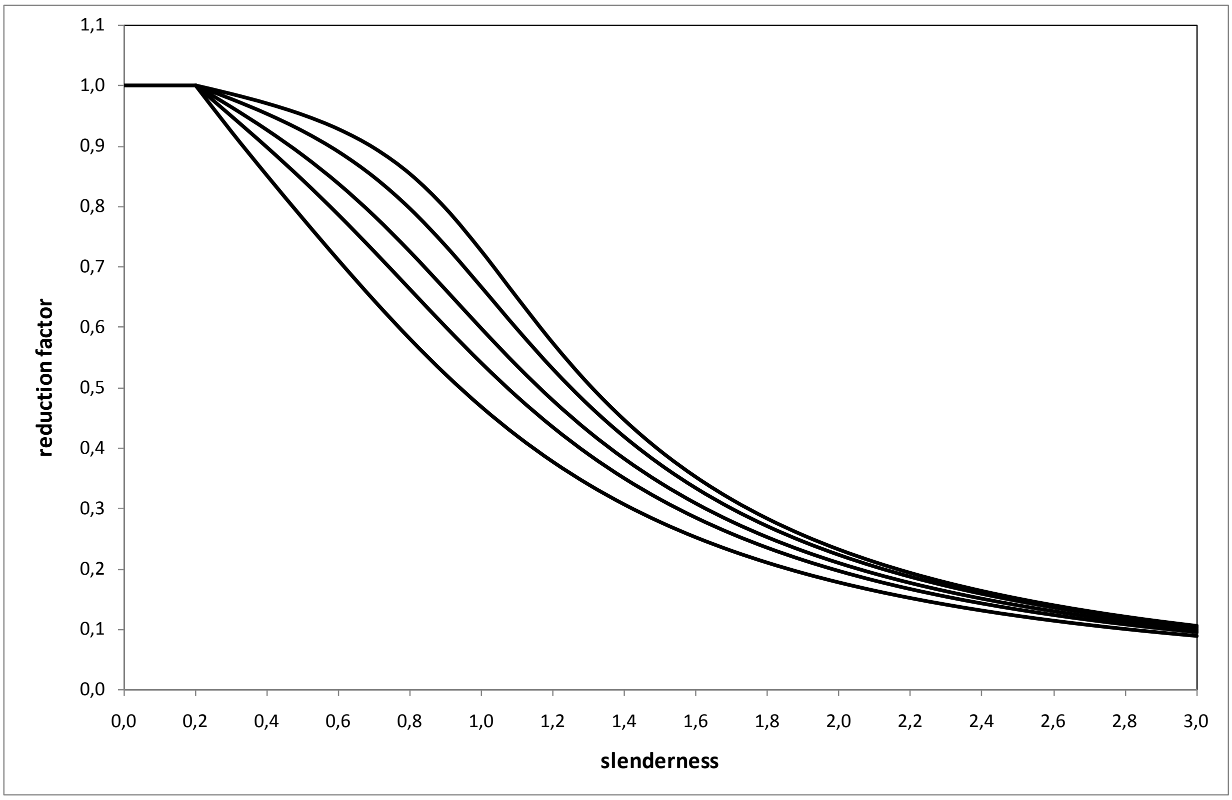

Fig. 4.5: Buckling curves [6]

The reduction factor is determined as follows

$$\chi = \frac{1}{\phi + \sqrt{\phi^2 - \lambda^2}} \leq 1 \tag{4.24}$$

$$\phi = \frac{1}{2} \cdot \left(1 + \alpha \cdot (\lambda - \lambda_0) + \lambda^2\right) \tag{4.25}$$

The slenderness λ_0 is a plateau value. If the slenderness of a component is less than λ_0 the yield strength is not reduced. According to EN 1993-1-1 for steel sections λ_0 = 0,2 has to be used.

This report may only be reproduced in an unabridged version. A publication in extracts needs our written approval.

In addition to the slenderness of the considered member the reduction factor depends on the imperfection factor α. Analogous to the equivalent geometrical imperfection this imperfection factor covers different imperfections (e.g. initial deformations, material imperfections, residual stresses). In EN 1993-1-1 the following imperfection factors are given for the different buckling curves.

buckling curve	imperfection factor
a	0,21
b	0,34
c	0,49
d	0,76

Fig. 4.6: Imperfection factors according to EN 1993-1-1

At load application areas there are additional imperfections, which mainly develop through sawing of the cut in the wall panel. During sawing often cracks occur between core and face, which disturb the bonding between core and face. Uneven cut edges result in contact imperfections and thus in stress peaks at the load application area (Fig. 4.7 and Fig. 4.8). This imperfections result in a further decrease of the load bearing capacity of the free edge.

Fig. 4.7: Cracks between core and face and uneven cut edge

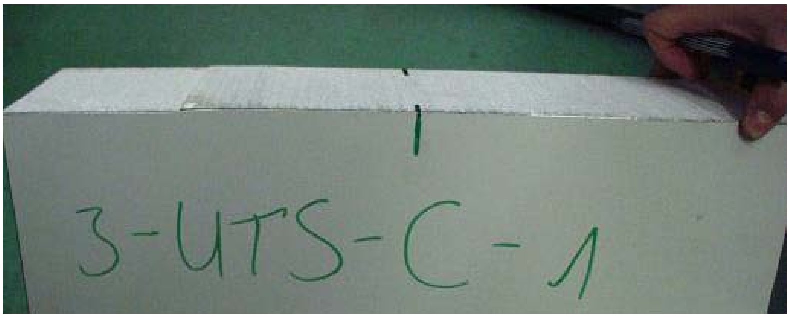

Fig. 4.8: Uneven cut edge

This report may only be reproduced in an unabridged version. A publication in extracts needs our written approval.

5 FE-models of numerical calculations

5.1 General

To investigate the load bearing behaviour and capacity of the load application area numerical calculations have been performed. The finite element program ANSYS has been used.
The face sheets of the panel were modelled with shell elements of type Shell 181. This element is defined by four nodes with three displacement degrees of freedom and three rotational degrees of freedom. It has bending, membrane and shear stiffness. As material behaviour, bilinear material equations were arranged (linear-elastic, ideal-plastic), i.e. after reaching the yield strength, yielding occurs without strain hardening.
The core layer of the panel was represented by volume elements of type Solid 185. This element has eight nodes with three displacement degrees of freedom. For the numerical investigations homogenous and isotropic core material was assumed.
As first step of the numerical calculation a linear buckling analysis is performed. As results of this analysis we get eigenvalue (elastic buckling load) and eigenmode. After the linear buckling analysis a non-linear analysis is performed to determine the load bearing capacity. In this analysis geometrical and material non-linearities are considered. So initial deformations must be taken into account. As initial deformation the first eigenmode determined in the linear buckling analysis is used.

5.2 Wrinkling in mid-span

To have reference values some investigations on the wrinkling stress in mid-span (face with infinite length) were performed. The model used for these calculations consists of a face sheet, which is supported by the core material. For sufficient thick panels both face sheets are independent of each other. So it is sufficient to represent only one face in the numerical model. The thickness of the core material has to be chosen as high that the deformations are gone down at the side opposite to the loaded face. The face is loaded by a normal force.
To take advantage of the symmetry only half of the model is represented in the FE-model. At one transverse edge symmetrical boundary conditions are used. Also at the longitudinal edges the model has symmetrical boundary conditions. At the side opposite to the loaded face the core is supported in thickness direction. The loaded edge of the face is supported in thickness direction and rotations are restraint. Because of the clamped edge failure occurs in mid-span. In the following figures transverse and longitudinal section of the model are shown.

This report may only be reproduced in an unabridged version. A publication in extracts needs our written approval.

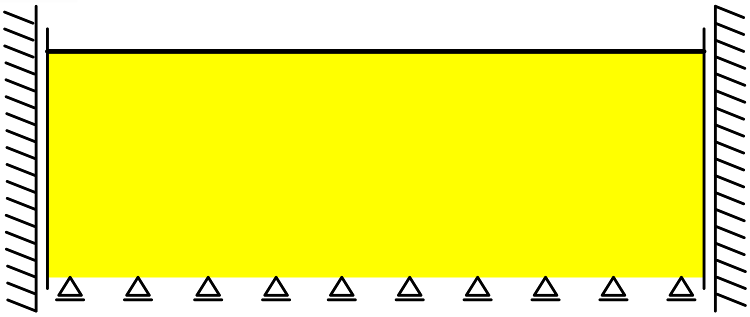

Fig. 5.1: Transverse section of model

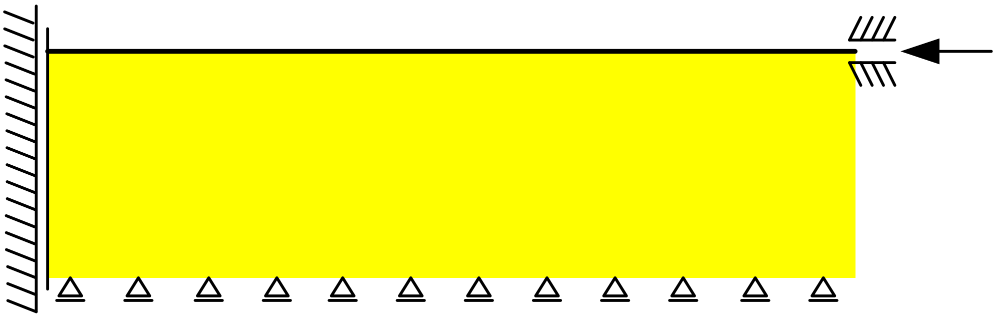

Fig. 5.2: Longitudinal section of model

Depending on the stiffness of face and core the length of the buckling waves, which cause the lowest eigenvalue, differs. To make sure that this buckling length can occur, for each model an appropriate length has to be chosen. For the calculations in the report at hand the length of the model was six times the length of a buckling wave according to formula (4.8).

This report may only be reproduced in an unabridged version. A publication in extracts needs our written approval.

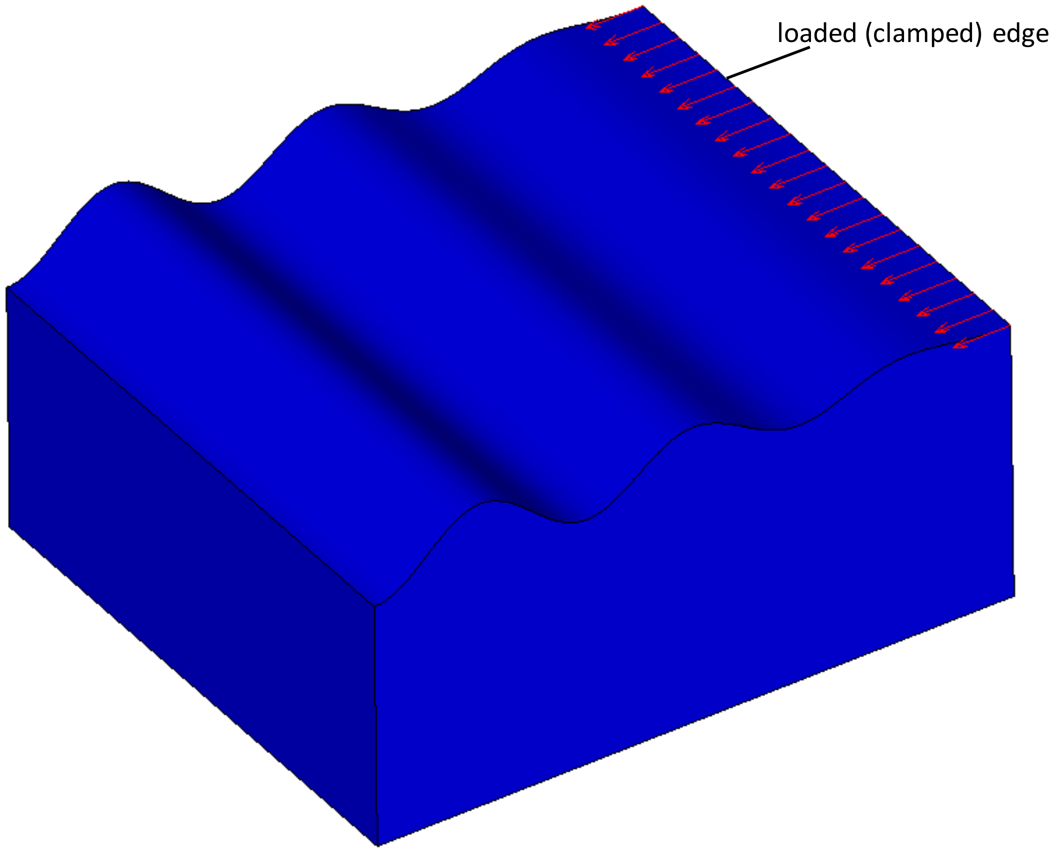

Fig. 5.3: **FE-model for investigations on wrinkling in mid-span (first eigenmode, boundary conditions are not shown)**

5.3 Crippling at load-application area

Like the model for calculation of the wrinkling stress in mid-span the model for investigations on the crippling stress consists of a face sheet, which is supported by the core material. In contrast to the model given in the previous section the loaded edge is not supported. The normal force is introduced into a free edge.

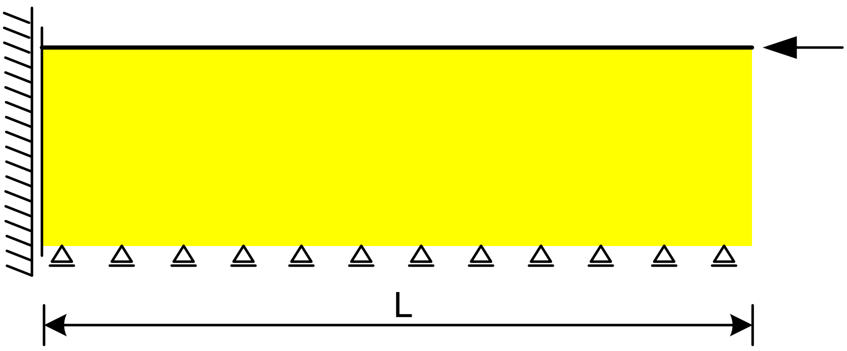

Fig. 5.4: **Longitudinal section of model with free edge**

For sufficient long models there is no influence of the length L on the load bearing behaviour and capacity of the loaded edge. So in a preliminary investigation the length of the model has

This report may only be reproduced in an unabridged version. A publication in extracts needs our written approval.

been chosen in a way that there is no influence of the length on the load bearing capacity of the edge. The face can be regarded as a semi-infinite plate.

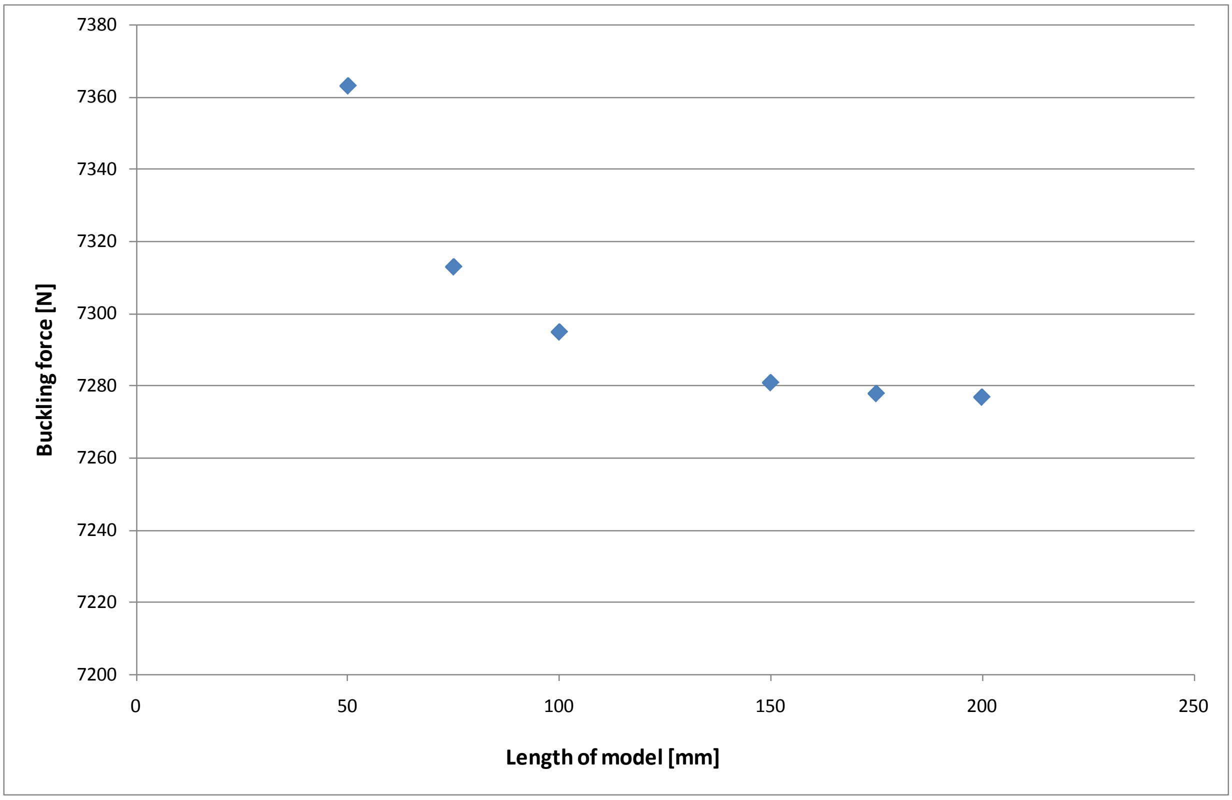

Fig. 5.5: Influence of length of the model on buckling load

This report may only be reproduced in an unabridged version. A publication in extracts needs our written approval.

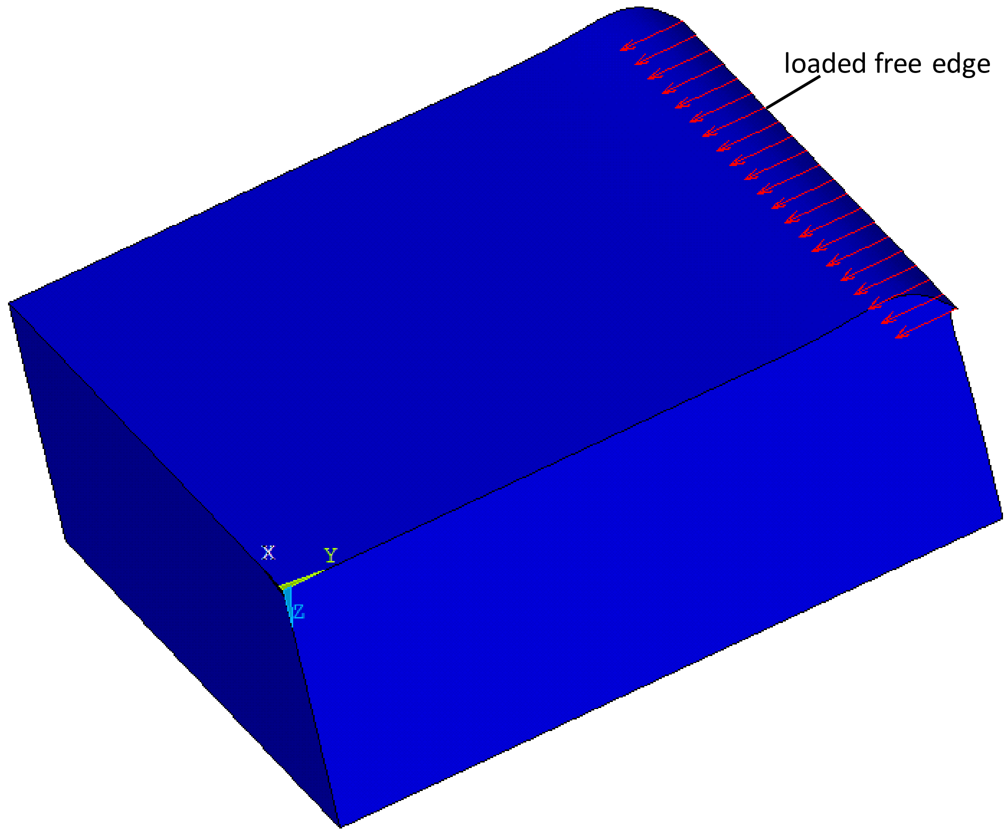

Fig. 5.6: **FE-model for investigations on crippling of the free edge (first eigenmode, boundary conditions are not shown)**

6 Wrinkling stress in mid-span

6.1 Introduction

To have a reference value some investigations on the wrinkling stress in mid-span have been performed. For the numerical investigations the FE-model described in section 5.2 has been used. As imperfection the first eigenmode, which was determined in an elastic buckling analysis, was used. The amplitude of the pre-deformation has been chosen approximately according to the acceptable deviation from flatness according to section D.2.2 of EN 14509.
According to EN 14509 the deviation from flatness has to be lower than the following values:

measuring length	acceptable deviation from flatness
200 mm	0,6 mm
400 mm	1,0 mm
700 mm	1,5 mm

Tab. 6.1: **Acceptable deviation from flatness according to EN 14509**

If these values are converted in amplitudes per length a_w of a buckling wave (cf. Fig. 6.1), we get as imperfections $a_w/176$, $a_w/200$ and $a_w/233$.

This report may only be reproduced in an unabridged version. A publication in extracts needs our written approval.

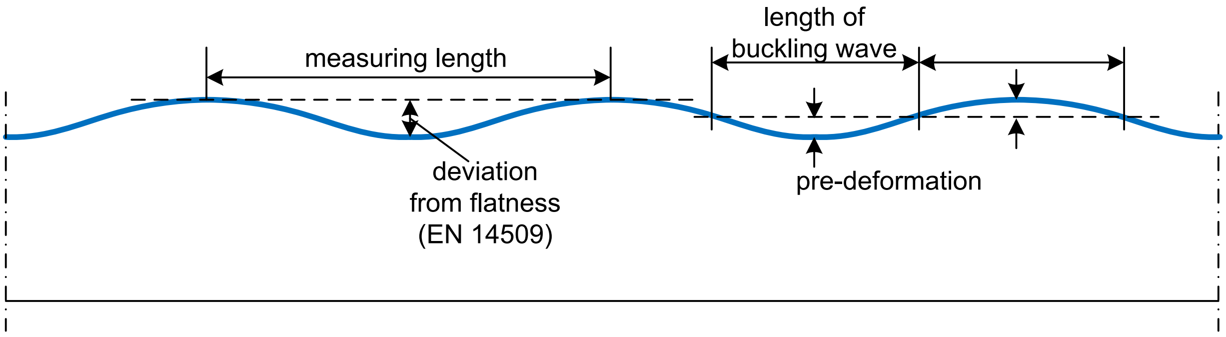

Fig. 6.1: Deviation from flatness and pre-deformation

According to the buckling curves of EN 1993-1-1 the following pre-deformations have to be used.

buckling curve	pre-deformation
a	L/300
b	L/250
c	L/200
d	L/150

Tab. 6.2: Pre-deformation according to EN 1993-1-1

The pre-deformations according to buckling curve b, c and d approximately correspond to the acceptable deviations from flatness given in EN 14509. So these values have been chosen for the following investigations.

6.2 Numerical investigations

By numerical calculations the ultimate stress (wrinkling stress) was determined. Within the calculations the thickness and the yield strength of the face and the material parameters of the core were varied. So the wrinkling stress σ_w was determined for different slenderness's. Based on the wrinkling stress σ_w, which was numerically determined, the reduction factor was determined.

$$\chi_w = \frac{\sigma_w}{f_{y,F}} \leq 1 \qquad (6.1)$$

In the following diagram the reduction factors are given as a function of the slenderness of the face. All parameters used for the calculations as well as the results are given in Annex 1.

This report may only be reproduced in an unabridged version. A publication in extracts needs our written approval.

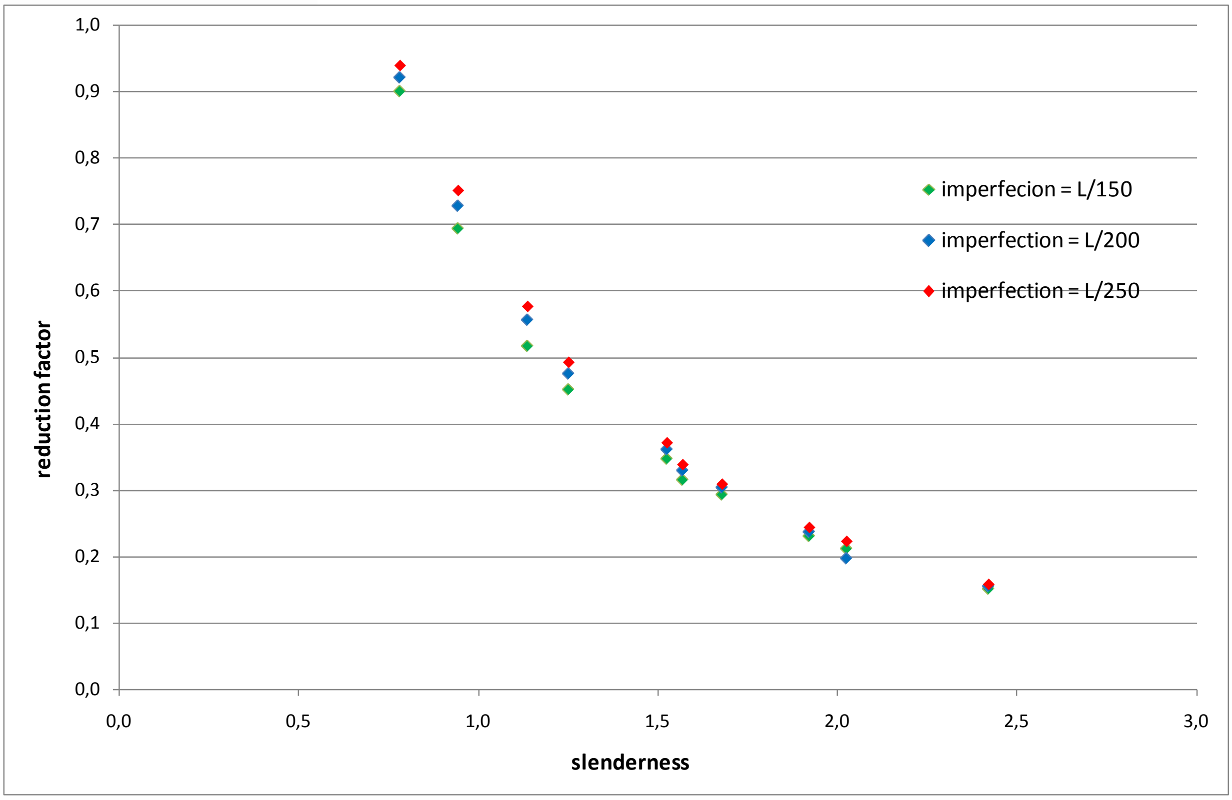

Fig. 6.2: **Reduction factors determined by numerical calculation**

In the following figures the results of the numerical calculations are compared to the buckling curves according to EN 1993-1-1 (blue curves). The buckling curves have been adjusted to have curves, which fit to the results of the numerical calculation (black curves). This has been done be an adjustment of the slenderness λ_0 to 0,7.

This report may only be reproduced in an unabridged version. A publication in extracts needs our written approval.

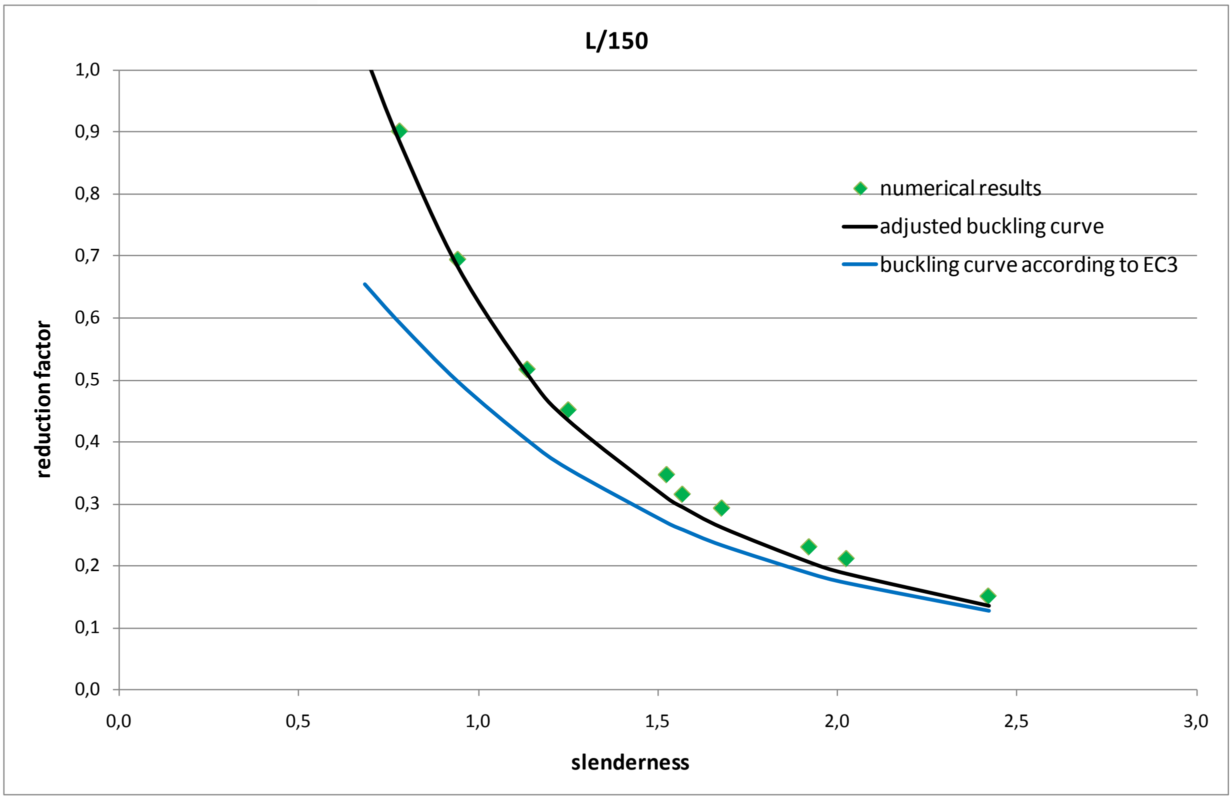

Fig. 6.3: **Buckling curves for L/150**

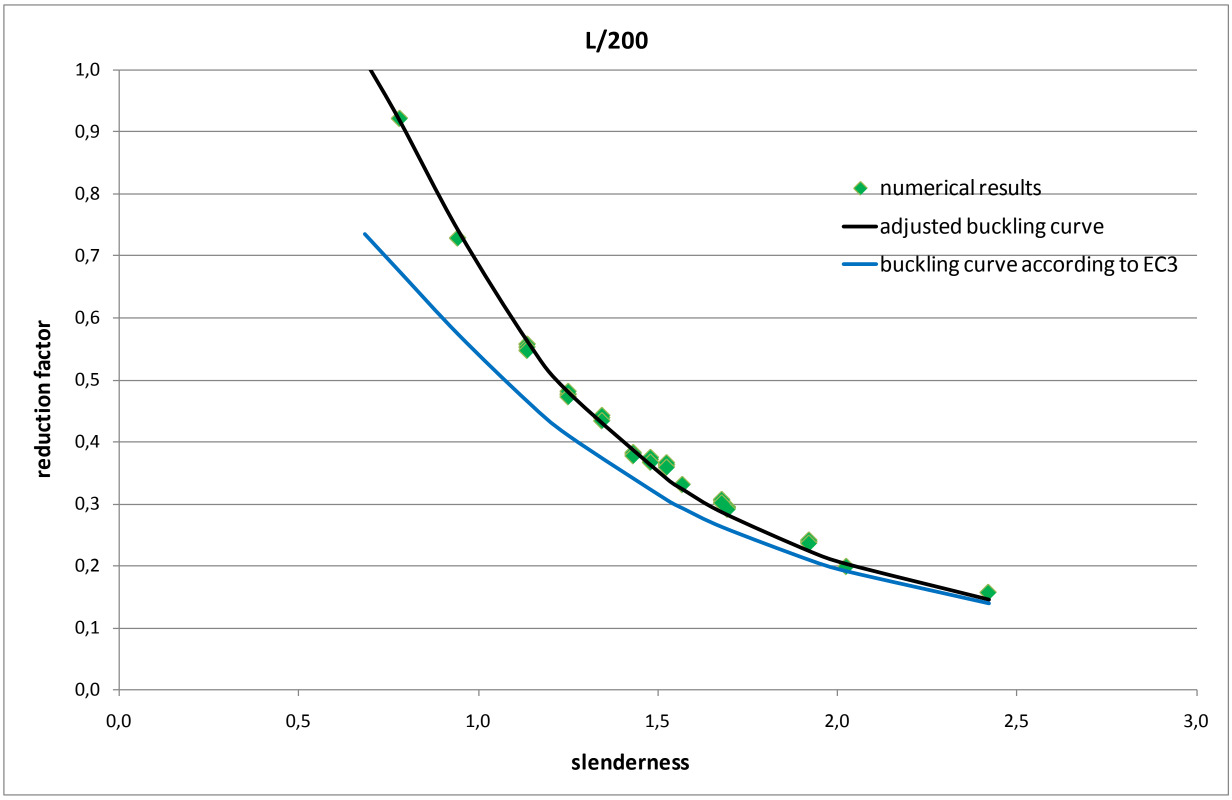

Fig. 6.4: **Buckling curves for L/200**

This report may only be reproduced in an unabridged version. A publication in extracts needs our written approval.

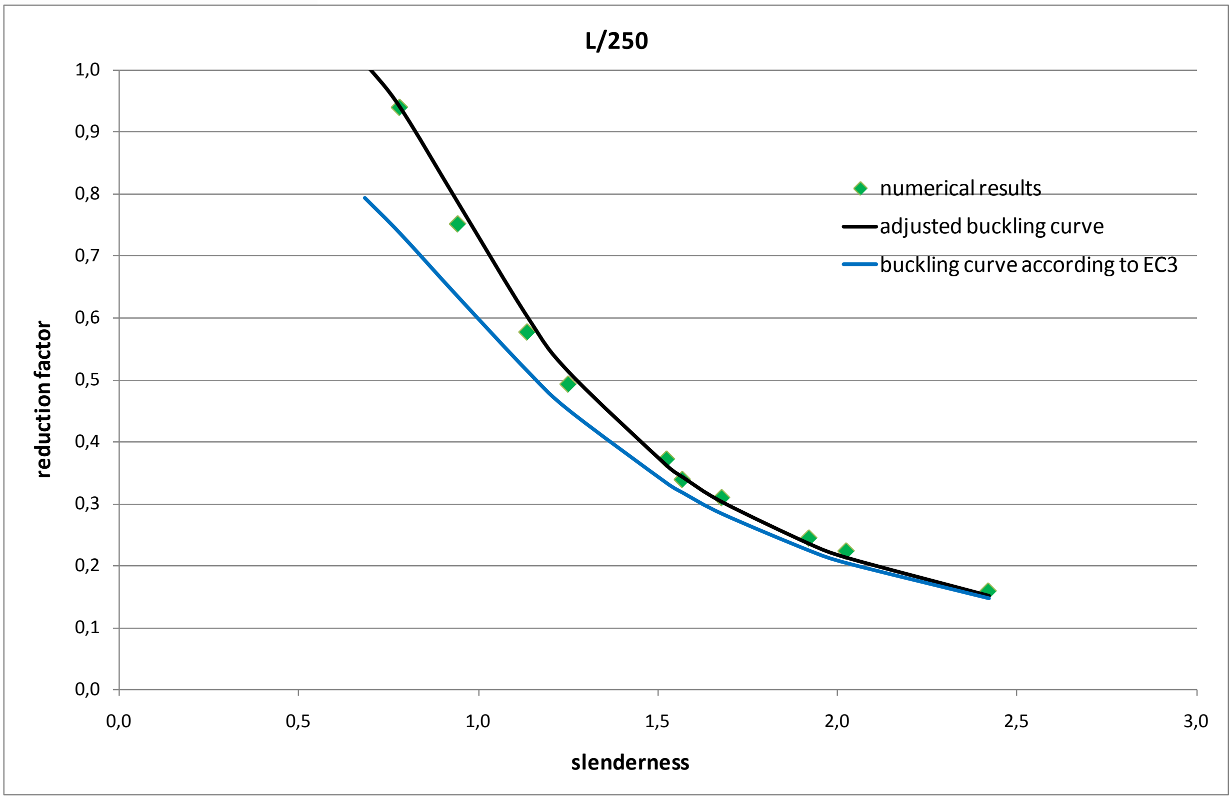

Fig. 6.5: Buckling curves for L/250

In several publications [12], [13] for the faces of sandwich panels with polyurethane foam core a pre-deformation of $a_w/500$ is suggested as a realistic value. Therefore for this imperfection numerical calculations have been performed and the imperfection factor α has been determined. It was assumed that the slenderness λ_0 is a constant value and thus can also be used for this case. The imperfection factor α = 0,21 was determined. In the following diagram the results of the numerical calculation and the corresponding buckling curve are presented.

This report may only be reproduced in an unabridged version. A publication in extracts needs our written approval.

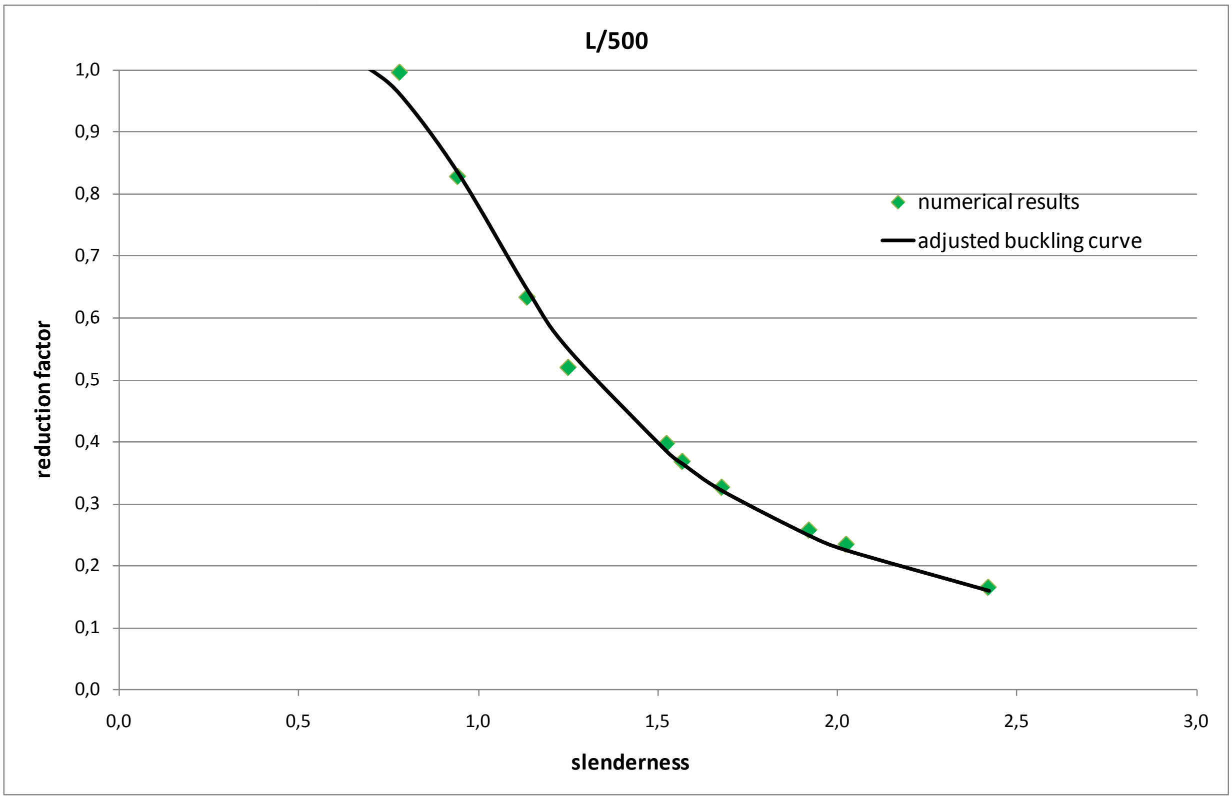

Fig. 6.6: **Buckling curve for L/500**

6.3 Conclusion

So if the imperfection factor for the considered panel would be known, the wrinkling stress of a flat or lightly profiled sandwich panel could be determined by calculation using buckling curves. In dependence of the equivalent geometrical imperfection (pre-deformation) the imperfection factors given in EN 1993-1-1 can be used. For a pre-deformation of L/500, which is according to [12] and [13] a realistic value for the face of a sandwich panel with a core made of polyurethane, the imperfection factor α = 0,21 can be used. In comparison to EN 1993-1-1 the slenderness λ_0 was adjusted to $\lambda_0 = 0,7$.

To use buckling curves for determination of the wrinkling stress by calculation, the imperfection factor α of the considered panel would need to be known. This factor depends on imperfections resulting from the production process as well as on the quality of the bond between core and face. So the imperfection factor should be determined by tests, i.e. the wrinkling stress is determined by testing and subsequently the imperfection factor is recalculated using formula (6.2). In the following this factor will be used to consider imperfections and quality of the bond between core and face also for the determination of the crippling stress of a free edge.

$$\alpha = \frac{1 + \chi_w \cdot \lambda_w^2 \cdot (\chi_w - 1) - \chi_w}{\chi_w \cdot (\lambda_w - \lambda_0)} \geq 0,21 \qquad (6.2)$$

This report may only be reproduced in an unabridged version. A publication in extracts needs our written approval.

7 Crippling of free edge

Numerical calculations have been performed to determine the crippling stress of a free edge, which is subjected to compression forces. The model described in section 5.3 has been used. As for the investigations on wrinkling in mid-span the first eigenmode, which was determined by an elastic buckling analysis, was used as geometrical imperfection. The same initial deformations have been chosen as for the investigations on the wrinkling stress in mid-span (L/150, L/200, L/250 and L/500). In the numerical calculation the ultimate stress and based on this the reduction factor was determined. All parameters used for the calculations as well as the results are given in Annex 2. The reduction factors determined by numerical calculations are compared to the buckling curves determined in the previous section (Fig. 7.1 to Fig. 7.4).

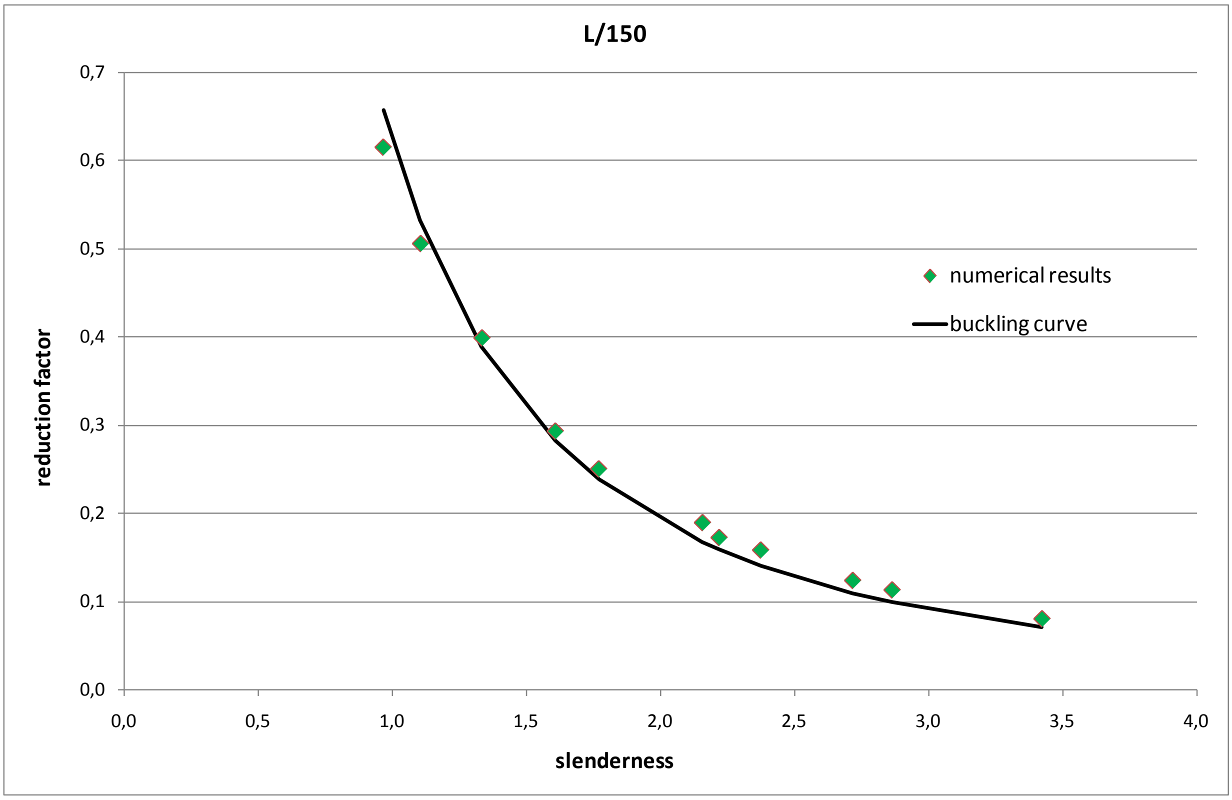

Fig. 7.1: Numerical results and buckling curve for L/150

This report may only be reproduced in an unabridged version. A publication in extracts needs our written approval.

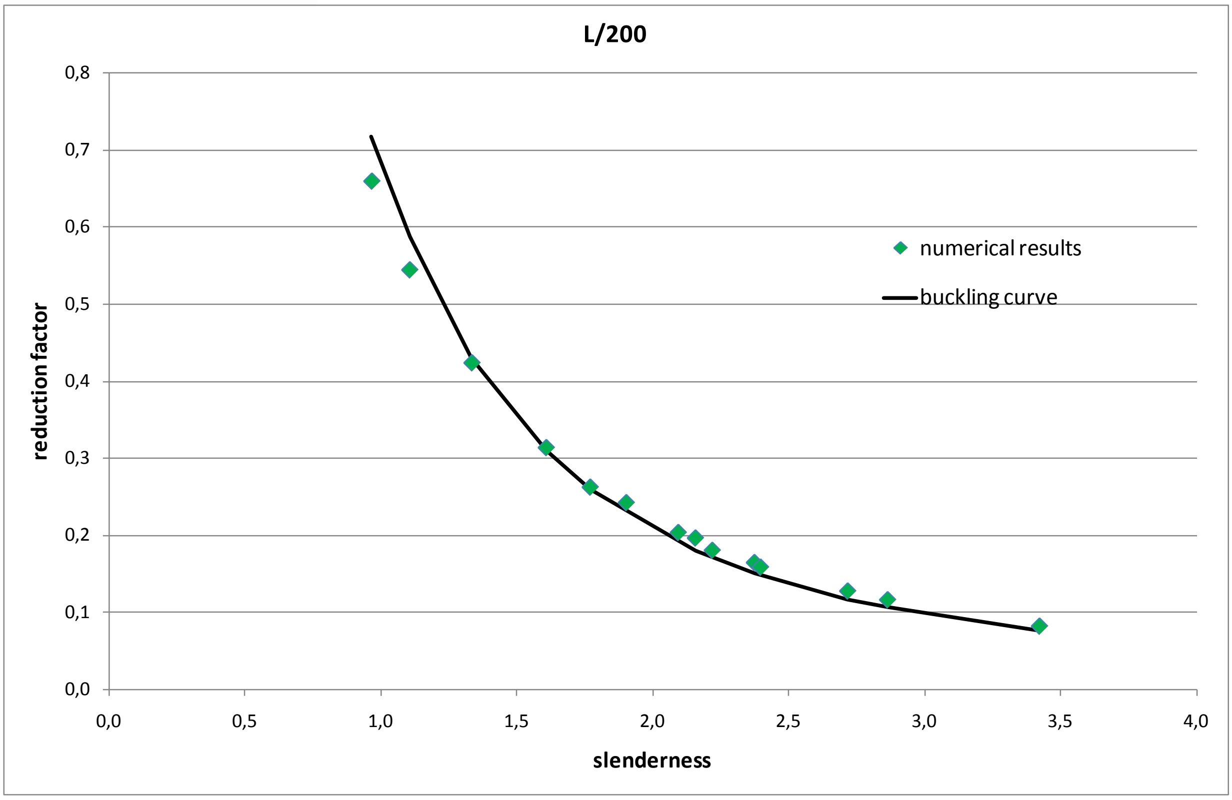

Fig. 7.2: Numerical results and buckling curve for L/200

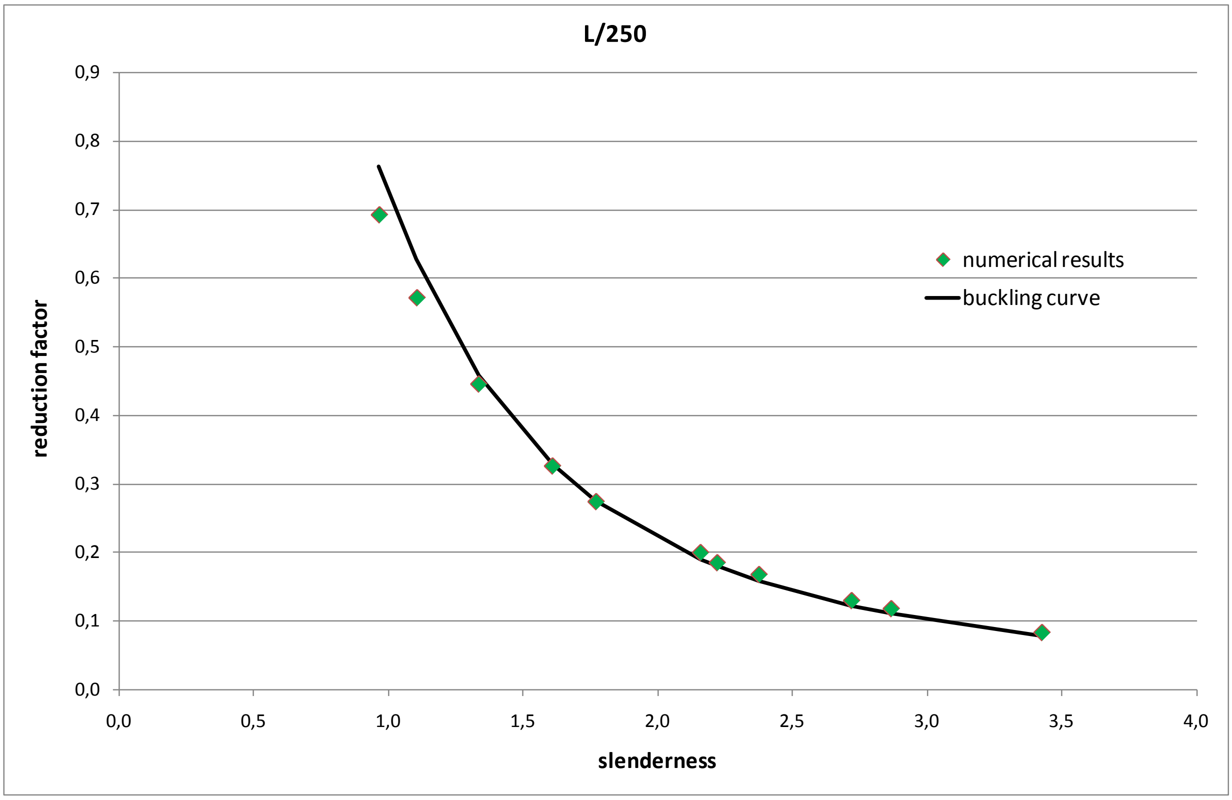

Fig. 7.3: Numerical results and buckling curve for L/250

This report may only be reproduced in an unabridged version. A publication in extracts needs our written approval.

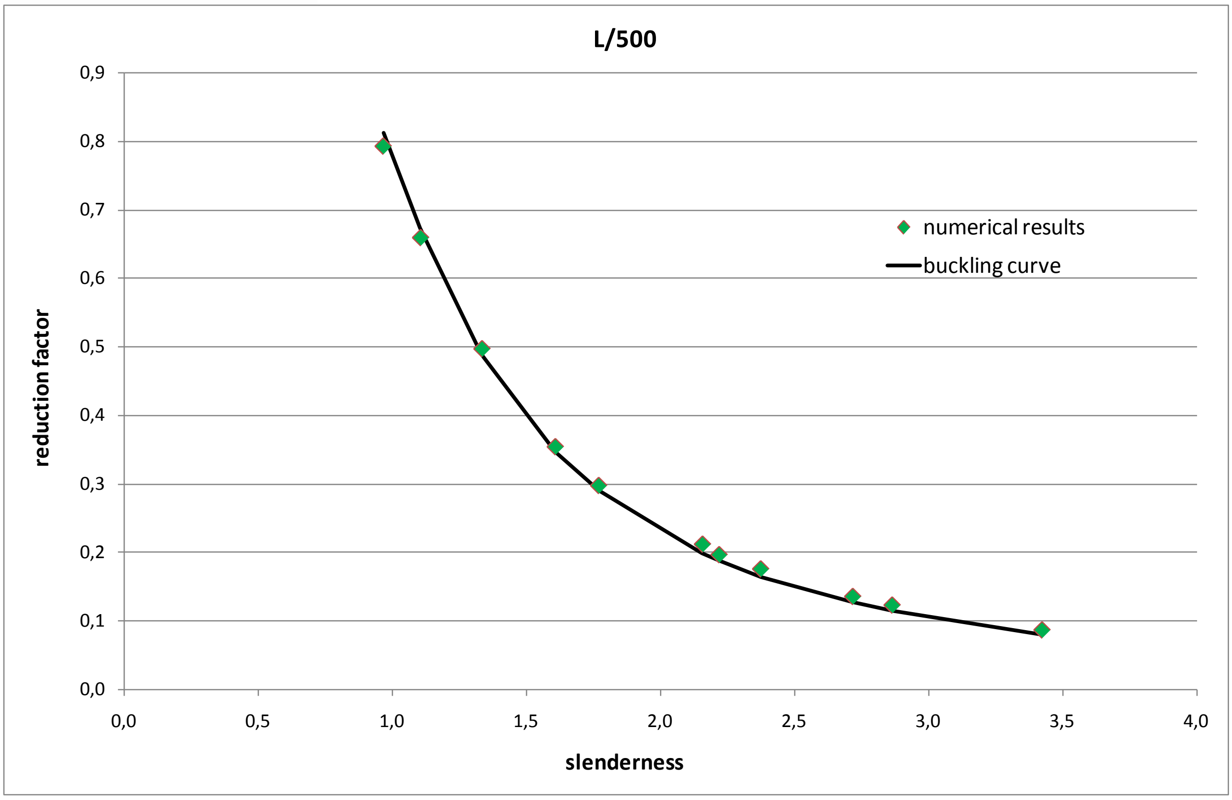

Fig. 7.4: Numerical results and buckling curve for L/500

The buckling curves determined for calculation of wrinkling stress in mid-span are also suitable for determination of the crippling stress of a free edge.

In addition to the imperfections, which are considered in the buckling curve by the imperfection factor α, at the free edge there are additional imperfections. From sawing of the edge cracks between core and face may occur. If the cut edge is uneven, the load is not introduced constantly over the width of the panel. Both things may decrease the load bearing capacity of the load application area. The influence of these further imperfections is investigated in the following section.

8 Consideration of further imperfections

If the load bearing capacity of a load application detail is determined by calculation with buckling curves (cf. section 7) an equivalent pre-deformation of the face is considered. This includes only the imperfections, which are also available in mid-span of the panel. Further imperfections as cracks between core and face and uneven cut edges cause an additional decrease of the load bearing capacity. This was investigated by evaluation of the tests, which are described in section 3. Because both kinds of test (direct introduction of the load and tests on corner details) showed no significant difference of the load bearing capacity, in the following all results are evaluated together.

To determine the influence of the imperfections caused by sawing of the edge the load bearing capacity of a panel without these imperfections must be known. The ultimate stress of a

This report may only be reproduced in an unabridged version. A publication in extracts needs our written approval.

panel with a perfect cut edge can be determined by the buckling curves given above. But to use the buckling curves the imperfection factor α for the considered panel must be known.
To determine the imperfection factor the wrinkling stress determined by tests (cf. Tab. 3.5) is used. From this wrinkling stress the imperfection factor was recalculated (Tab. 8.1). In doing so the mean value of the wrinkling stresses determined for one type of panel was used. Also for the other material factors the mean values determined by tests have been used. For some panels the calculated imperfection factor is lower than 0,21, what corresponds to an imperfection of L/500. In these cases the imperfections factor α = 0,21 was used as a minimum value.

type of panel	wrinkling stress (mean values) [N/mm^2]	yield strength [N/mm^2]	reduction factor	slenderness λ_w of the face	imperfection factor α
A	201	358	0,561	1,311	≤ 0,21
B	201	403	0,499	1,446	≤ 0,21
C	176	409	0,430	1,600	≤ 0,21
E	196	467	0,281	1,253	2,60
Details of determination of the imperfection factor are given in Annex 3.					

Tab. 8.1: Imperfection factors determined from wrinkling tests

With the imperfection factor determined from the wrinkling stress in mid-span the crippling stress σ_c* of the free edge is calculated (Tab. 8.2). These calculated values consider only the imperfections, which are also available at mid-span; they require a perfect cut edge. Further imperfections, which are caused by cutting of the edge (e.g. contact imperfections), are not considered.

type of panel	yield strength [N/mm^2]	imperfection factor α	slenderness λ_c of the face	reduction factor	crippling stress σ_c* [N/mm^2]
A	358	0,21	1,854	0,265	95,0
B	403	0,21	2,044	0,220	88,7
C	409	0,21	2,262	0,181	74,1
E	467	2,60	1,772	0,155	72,6
Details of determination of the crippling stress σ_c* are given in Annex 3.					

Tab. 8.2: Crippling stresses

To evaluate the influence of additional imperfections, which are caused by cutting of the edge and therefore are only available at the load application area, the calculated values of the crippling stress σ_c* (Tab. 8.2) are compared to the ultimate stresses determined in the tests. In some tests the ultimate stress was in the range of or even slightly higher than the elastic buckling stress. These results were not taken into account in the evaluation of the tests. In

This report may only be reproduced in an unabridged version. A publication in extracts needs our written approval.

Tab. 8.3 for each test the reduction factor ($\sigma_{c,test}/\sigma_{c,cal}$) is determined. In doing so the crippling stresses (local buckling of a free edge) determined in the tests (Tab. 3.7 to Tab. 3.14) are divided by the respective calculated values σ_c* given in Tab. 8.2. This reduction factor describes the decrease of the load bearing capacity caused by imperfections resulting from cutting of the edge. By a statistical evaluation the characteristic value of the reduction factor was determined to $\sigma_{c,test}/\sigma_{c,cal}$ = 0,54.

panel type A		panel type B		panel type C		panel type E	
ultimate stress (tests) [N/mm²]	$\sigma_{c,test}/\sigma_{c,cal}$	ultimate stress (tests) [N/mm²]	$\sigma_{c,test}/\sigma_{c,cal}$	ultimate stress (tests) [N/mm²]	$\sigma_{c,test}/\sigma_{c,cal}$	ultimate stress (tests) [N/mm²]	$\sigma_{c,test}/\sigma_{c,cal}$
59,5	0,627	63,1	0,712	58,3	0,787	63,7	0,878
74,5	0,784	70,5	0,794	46,9	0,633	64,9	0,894
74,6	0,785	63,7	0,718	47,7	0,643	68,3	0,940
66,5	0,700	64,3	0,725	57,9	0,782	64,7	0,891
64,8	0,682	70,2	0,791	34,2	0,461	52,3	0,720
78,0	0,821	92,1	1,039	37,4	0,505	60,5	0,833
66,7	0,702	66,9	0,754	39,3	0,530	48,1	0,662
85,9	0,904	50,3	0,567	56,0	0,756	42,3	0,583
79,4	0,836	53,2	0,599	33,7	0,455	61,4	0,845
73,7	0,776	48,6	0,548	42,1	0,568	45,7	0,630
70,1	0,738	66,1	0,746	53,2	0,718	58,7	0,809
66,6	0,701	79,2	0,893			53,6	0,739
91,5	0,963	67,6	0,762			64,9	0,894
85,5	0,900	86,2	0,972			47,9	0,660
		84,4	0,952			57,1	0,786
		84,3	0,950			67,2	0,925
		67,3	0,759			55,3	0,762
		60,5	0,682			57,5	0,792
		63,6	0,717			50,9	0,701
		67,4	0,760			46,4	0,639
		80,9	0,912			47,5	0,654
		78,4	0,884			55,4	0,763
		61,9	0,698			41,7	0,574
		65,2	0,735			41,6	0,573
mean value of $\sigma_{c,test}/\sigma_{c,cal}$							0,75
characteristic value of $\sigma_{c,test}/\sigma_{c,cal}$							0,54

Tab. 8.3: Evaluation of tests on load application details

This report may only be reproduced in an unabridged version. A publication in extracts needs our written approval.

So to determine the crippling stress of the free edge the imperfection factor α of the panel has to be known. This factor is determined based on the wrinkling stress in mid-span (cf. formula (6.2)). (To determine the wrinkling stress tests are necessary.) With the imperfection factor the crippling stress σ_c^* of a perfectly cut edge is determined by buckling curves (formulae (4.24) and (4.25)). To consider further imperfection, which are caused by cutting of the edge, the crippling stress has to be decreased by the factor 0,54 to get the characteristic value or by 0,75 to get the mean value. In Fig. 8.1 for panel type E the crippling stresses determined by tests are compared to the calculated values.

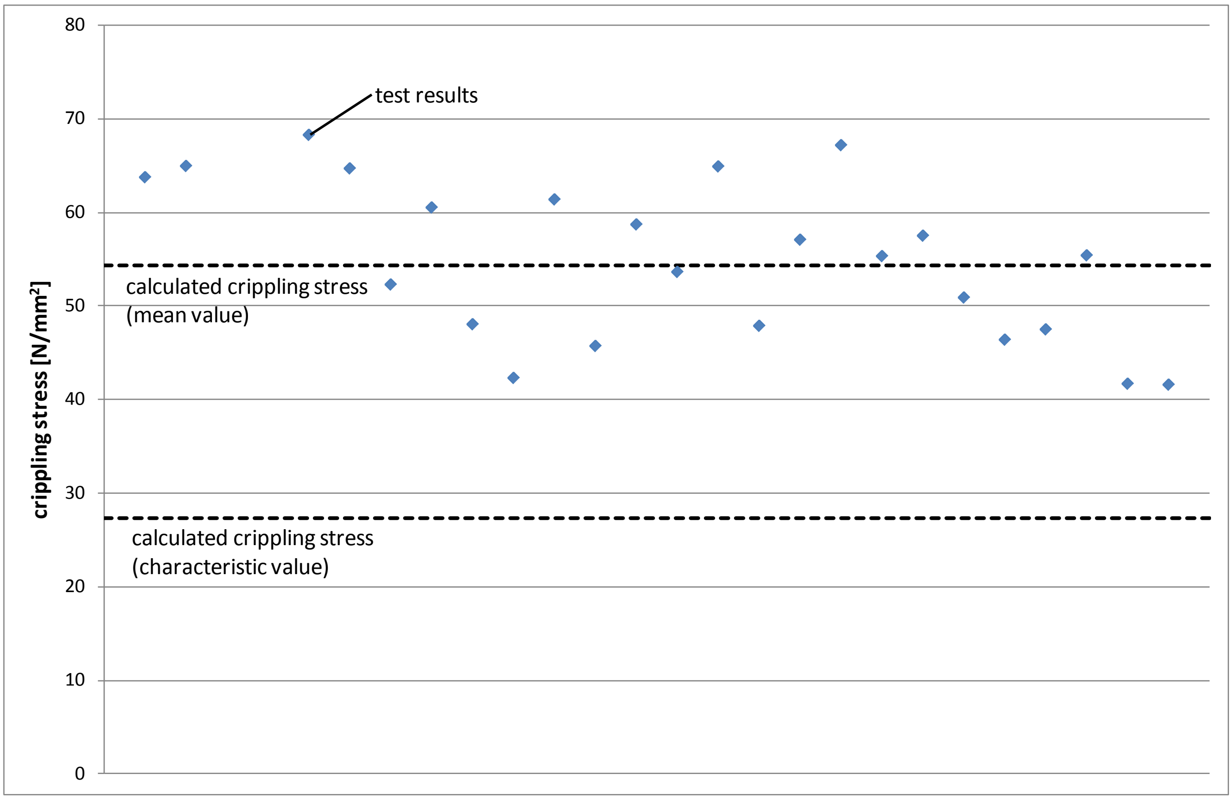

Fig. 8.1: Comparison of tests results and calculated values

Obviously imperfections caused by cutting of the edge reduce the load bearing capacity of the load application area significantly. So if sandwich panels are intended to introduce normal forces into the free edges of the face, special care should be taken, when cutting the panel. It should be avoided to damage the edges of the panel, i.e. the bond between core and face should not be destroyed. Furthermore it is important to have even cut edges to be able to introduce the loads constantly over the width of the panel.

9 Introduction of loads in both face sheets

In the tests and also in the numerical calculations the load was applied to one face of a sandwich panel only. But in practice there are also applications, which require applying loads to both faces of a panel, e.g. the roof introduces loads into an interior wall. For panels with a

This report may only be reproduced in an unabridged version. A publication in extracts needs our written approval.

sufficiently thick core (approx. 60 mm) both faces do not influence each other [15]. This is also shown by the tests on load application areas presented in section 3.2. For some samples both faces were tested one after the other. The results of the tests on samples with one face already destructed do not differ significantly from the tests on “new” samples.

The independent behaviour of both faces could also be shown with an additional test series. For these tests sandwich panels with a mineral wool core with thickness 60 mm have been used. Two tests with introduction of the load into both faces and two tests with introduction of the load into one face only have been performed (Fig. 9.1).

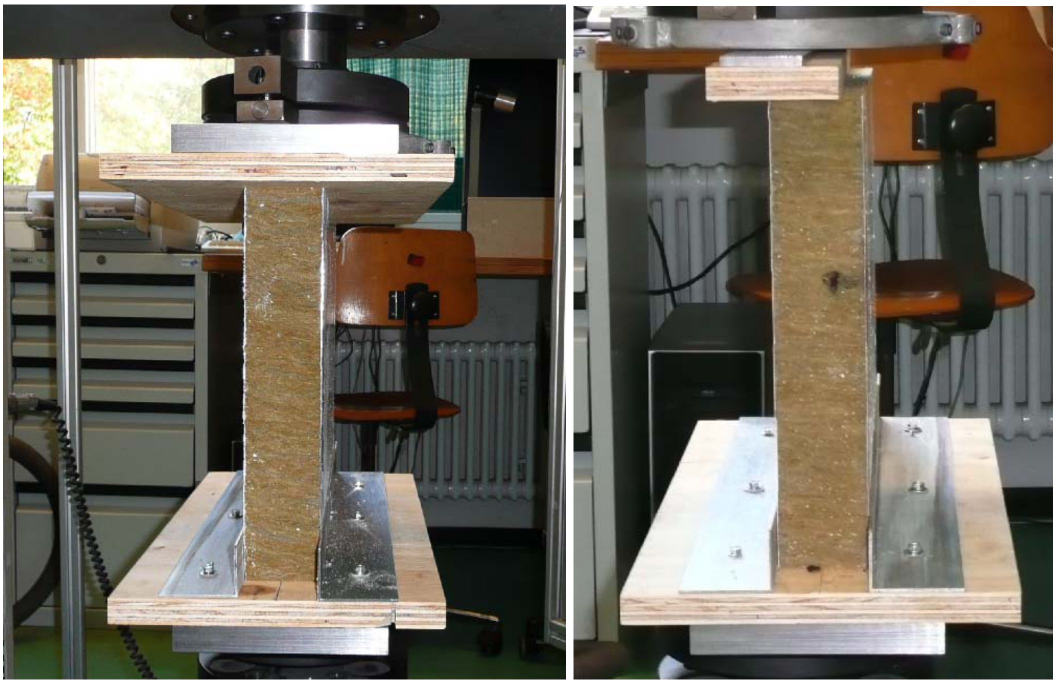

Fig. 9.1: Introduction of load into both faces and into one face

The results of the tests (ultimate loads) are given in Tab. 9.1.

introduction into both faces		introduction into one face	
No. 1	13,9 kN	No. 3	6,9 kN
No. 2	13,7 kN	No. 4	6,8 kN

Tab. 9.1: Ultimate loads

The results of test no. 3 and 4 (introduction of load into one face) are approximately half of the values of test no. 1 and 2 (introduction of load into both faces). So obviously, both faces do not depend from each other. For panels with loading of both faces a reduction of the load bearing capacity is not necessary.

This report may only be reproduced in an unabridged version. A publication in extracts needs our written approval.

10 Design of load application areas

To design the load application area of an axially loaded sandwich panel, where normal forces are introduced into the free edge of the panel, the following calculation procedure can be used.

The basis of the calculations is the wrinkling stress in mid-span. The wrinkling stress is determined be testing. Usually it can be found on the CE-mark of the sandwich panel or in approvals. Based on the wrinkling stress the imperfection factor α of the considered panel is calculated. As a minimum value α = 0,21 is used.

$$\alpha = \frac{1 + \chi_w \cdot \lambda_w^2 \cdot (\chi_w - 1) - \chi_w}{\chi_w \cdot (\lambda_w - \lambda_0)} \geq 0{,}21 \qquad (10.1)$$

with

reduction factor for wrinkling stress:

$$\chi_w = \frac{\sigma_w}{f_{y,F}} \qquad (10.2)$$

elastic buckling load (wrinkling):

$$\sigma_{cr,w} = \frac{3}{A_F} \cdot \sqrt[3]{\frac{2}{9} \cdot EI_F \cdot G_C \cdot E_C} \qquad (10.3)$$

slenderness for wrinkling:

$$\lambda_w = \sqrt{\frac{f_{y,F}}{\sigma_{cr,w}}} \qquad (10.4)$$

$$\lambda_0 = 0{,}7 \qquad (10.5)$$

With the imperfection factor the crippling stress σ_c* of the free edge is determined. This value only considers imperfections, which are available at the free edge as well as at mid-span. Further imperfections of the free edge, e.g. contact imperfections, are not considered.

$$\sigma_c^* = \chi_c \cdot f_{y,F} \qquad (10.6)$$

with

slenderness for crippling

$$\lambda_c = \sqrt{2} \cdot \lambda_w \qquad (10.7)$$

reduction factor for crippling stress

$$\chi_c = \frac{1}{\phi + \sqrt{\phi^2 - \lambda_c^2}} \leq 1 \qquad (10.8)$$

$$\phi = \frac{1}{2} \cdot \left(1 + \alpha \cdot (\lambda_c - \lambda_0) + \lambda_c^2\right) \qquad (10.9)$$

This report may only be reproduced in an unabridged version. A publication in extracts needs our written approval.

To consider also further imperfections of the free edge, e.g. uneven cut edges, which can cause contact imperfections, an additional reduction of the crippling stress has to be taken into account. From the stress σ_c* the characteristic value of the crippling stress is calculated to

$$\sigma_{c,k} = 0{,}54 \cdot \sigma_c^* \qquad (10.10)$$

To design the load application area the crippling stress has to be compared to the introduced normal stress σ_d.

$$\sigma_d \le \frac{\sigma_{c,k}}{\gamma_M} \qquad (10.11)$$

The introduced stress σ_d is a design value. By determination of this value load factors γ_F and combination coefficients Ψ have to be considered. They are given by national specifications, e.g. they can be found in EN 1990 [5] and the related national annex.

For sandwich panels the material factors γ_M represent the variability of the mechanical properties of the sandwich panel. They are determined by the results of initial type testing and factory production control. Because the failure mode of crippling of the free edge is related to wrinkling in mid-span, the material factors for wrinkling could also be used for the design of load application areas.

11 Load application details with glued cores

Especially for cooling chambers it is common practice to glue the cores of the panel at the connection between roof and wall. To investigate the influence of this additional connection tests on corner details with glued cores have been performed. A wall panel and a roof panel of the same type were glued with glue „OTTOCOLL® P84“ (polyurethane glue). The roof panel was loaded as single span beam. The test set up of the tests is shown in Fig. 11.1 and Fig. 11.2. The roof panel was supported by an additional hinged support and loaded by four line loads. During the test the reaction force F_2 at the hinged support and the deflection in mid-span at the lower face of the panel were measured.

This report may only be reproduced in an unabridged version. A publication in extracts needs our written approval.

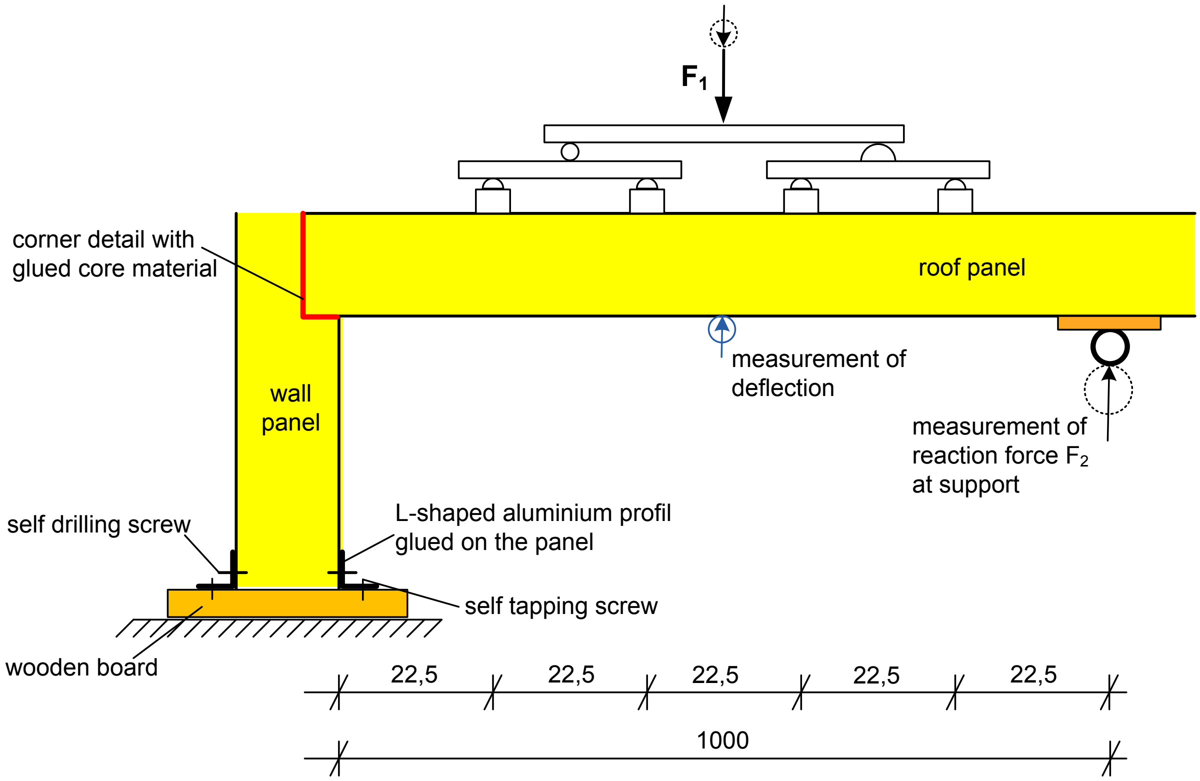

Fig. 11.1: **Test set-up**

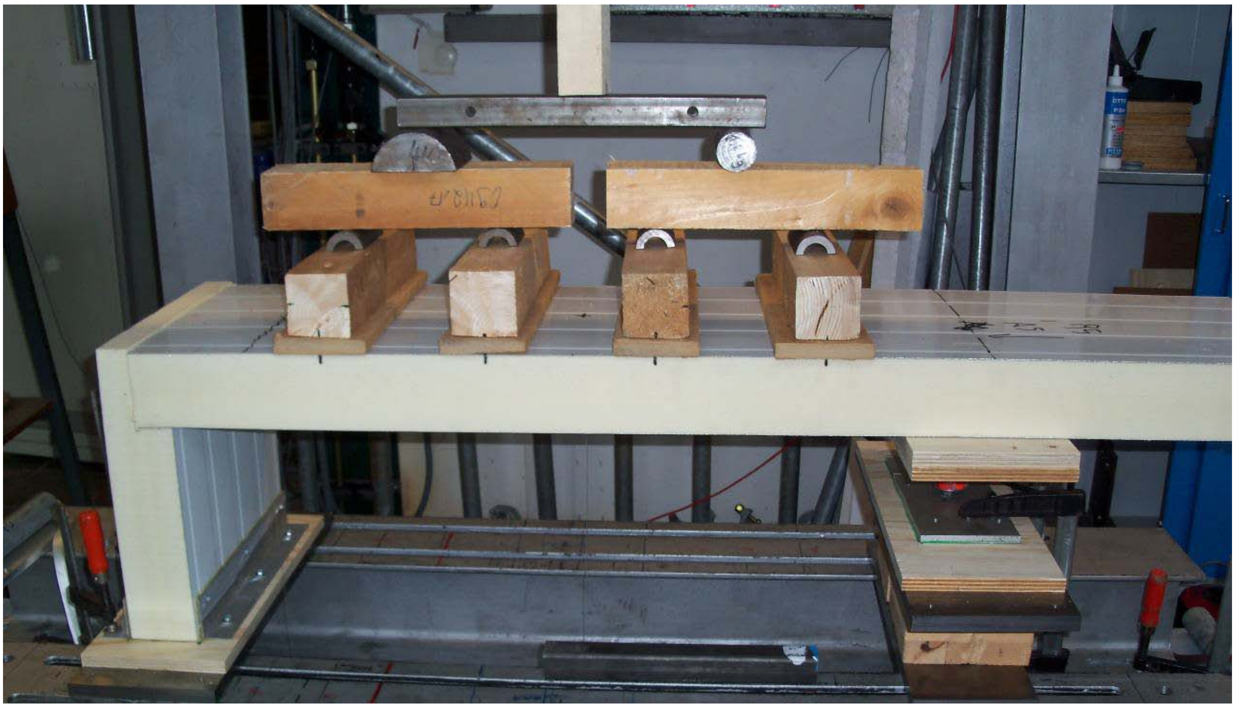

Fig. 11.2: **Test set-up**

In all tests failure did not occur in the wall but in the roof panel.

This report may only be reproduced in an unabridged version. A publication in extracts needs our written approval.

Fig. 11.3: Failure of roof panels

In the following table the results of the tests are summarised. The ultimate load F_1 (load introduced into roof panel) and F_2 (load at support) and the quotient of both values are given. The load-deflection curves of the tests are presented in Fig. 11.4 to Fig. 11.7.

type of panel	number of test	F_1 [kN]	F_2 [kN]	F_2/F_1
A	1	8,72	4,36	0,50
	2	10,79	5,50	0,51
	3	9,77	4,96	0,51
B	1	16,07	8,22	0,51
	2	15,44	7,72	0,50
	3	14,09	7,17	0,51
	4	15,59	7,94	0,51
	5	15,29	7,88	0,52
	6	16,11	8,39	0,52
C	1	8,34	3,99	0,48

Tab. 11.1: Test results

This report may only be reproduced in an unabridged version. A publication in extracts needs our written approval.

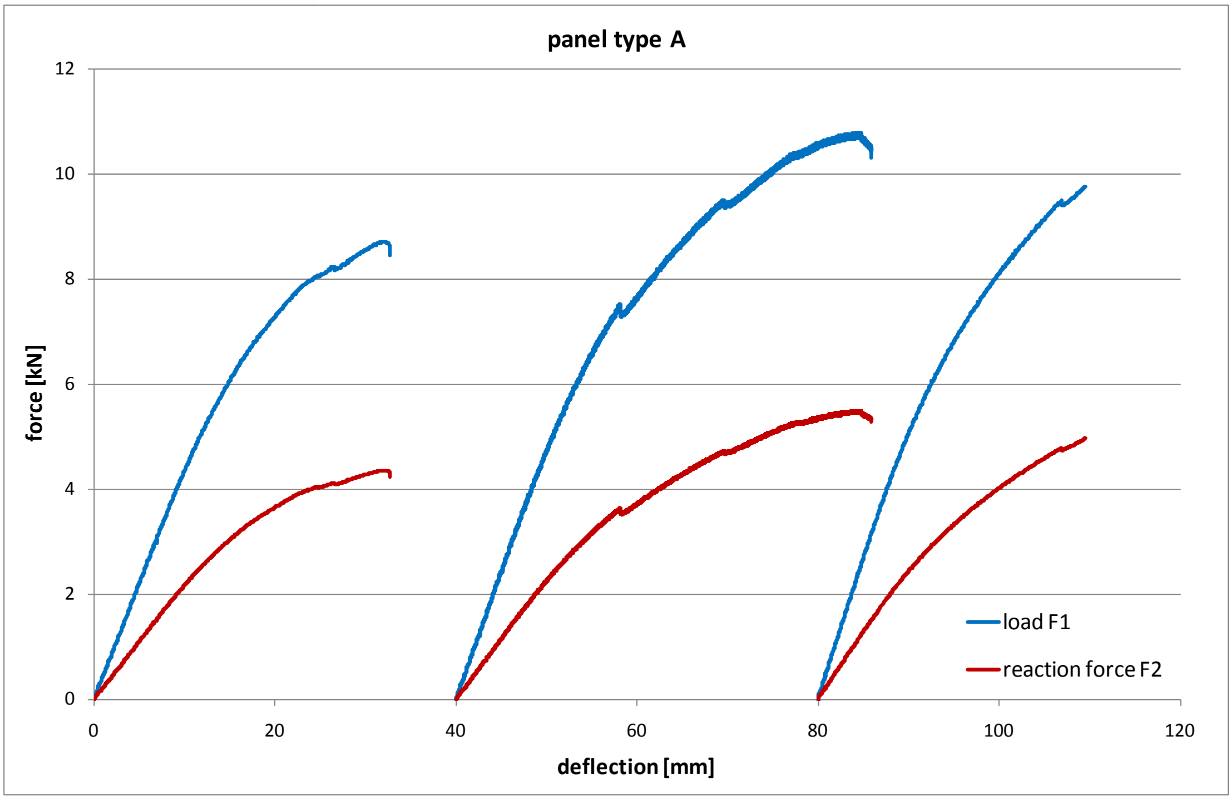

Fig. 11.4: Load-deflection curve – panel type A

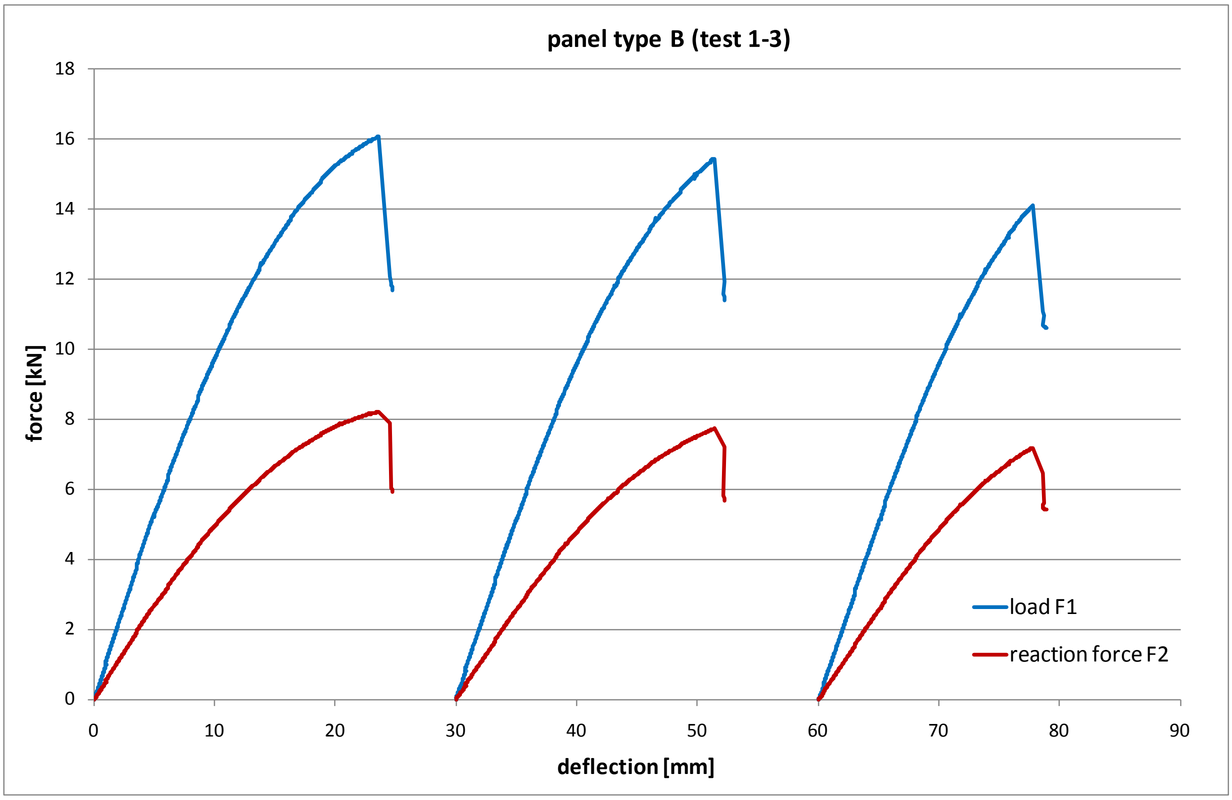

Fig. 11.5: Load-deflection curve – panel type B (test 1-3)

This report may only be reproduced in an unabridged version. A publication in extracts needs our written approval.

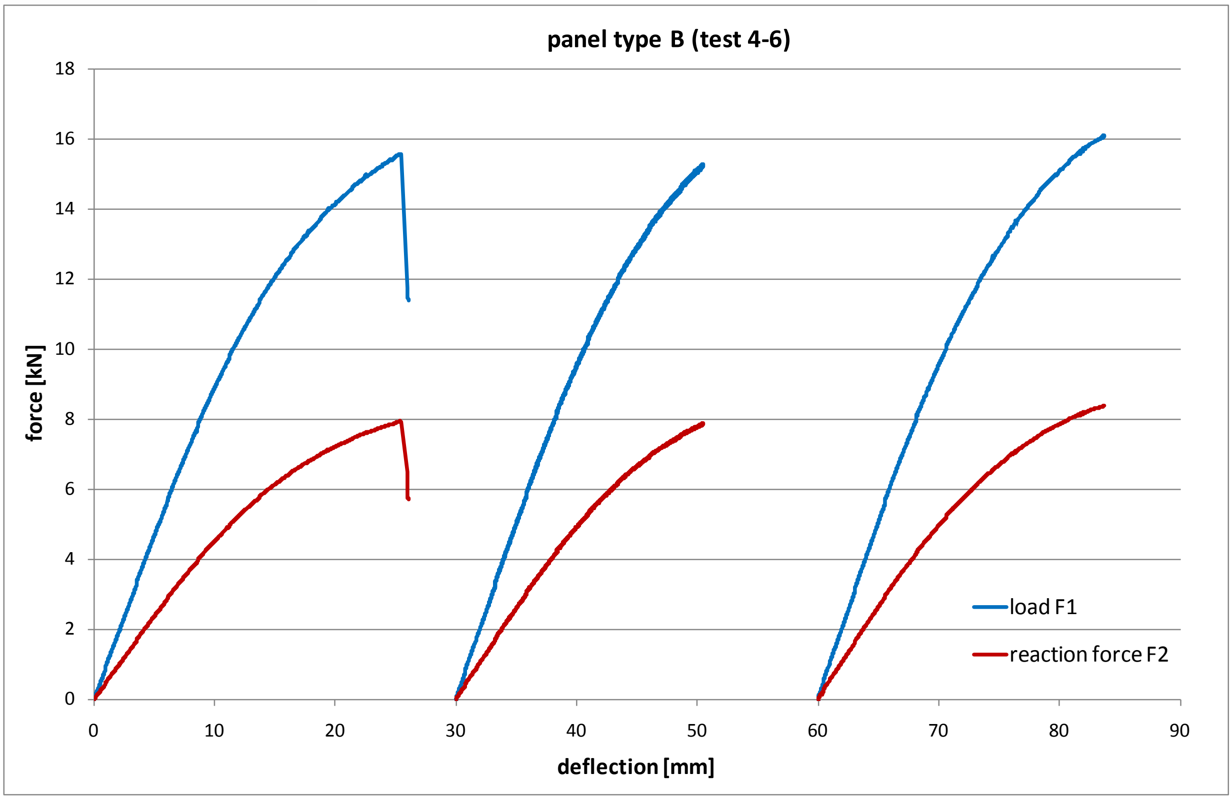

Fig. 11.6: Load-deflection curve – panel type B (test 4-6)

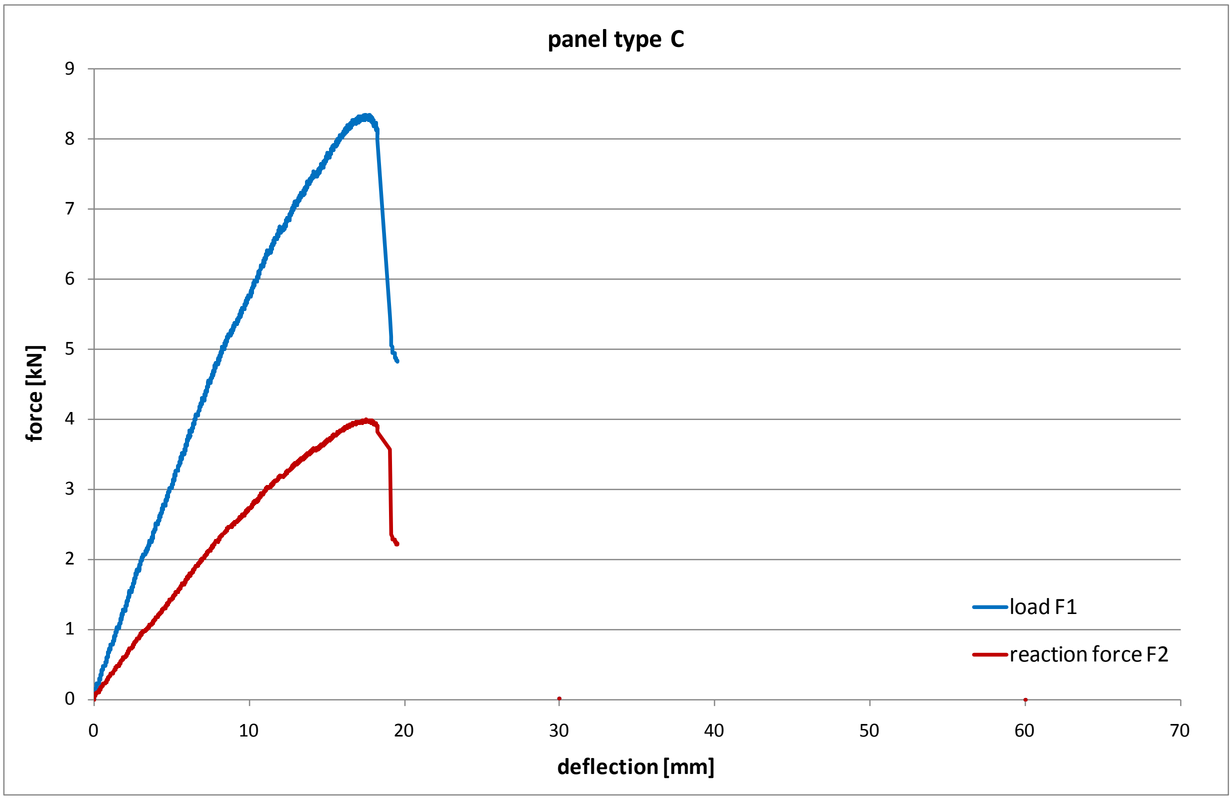

Fig. 11.7: Load-deflection curve – panel type C

If the load introduced into the roof panel and the force measured at the support are compared, it is obvious that half of the load is transferred to the hinged support and half of the load to the

This report may only be reproduced in an unabridged version. A publication in extracts needs our written approval.

inner face of the wall panel. So the connection between wall and roof can be regarded as hinged, no moments are transferred, even if the cores of wall and roof panel are bonded by gluing. The load from the roof is applied as normal force into the inner face of the wall panel.

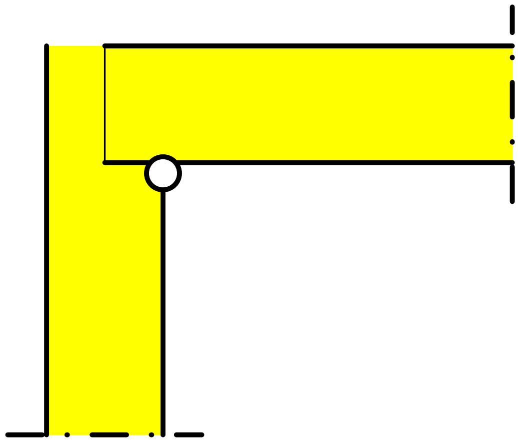

Fig. 11.8: Static system of connection between wall and roof

12 Summary

The common application of sandwich panels is enclosure of buildings. A new application is to apply sandwich panels without any load transferring substructure. In this new type of application the sandwich panels have to transfer loads and to stabilise the building. The wall panels transfer normal forces arising from the superimposed load from overlying roof or ceiling panels.

Within the framework of work package 3 of the EASIE project, design methods for axially loaded sandwich panels have been developed. In addition to the global load bearing behaviour [1] also the load application area, e.g. the connection between wall and roof, where normal forces are introduced by contact, has to be considered. In the report at hand a design procedure for the load application area of axially loaded sandwich panels is introduced. Based on the wrinkling stress in mid-span the ultimate stress of the load application area can be determined. The method has the advantage, that only values, which are also used to design sandwich panels subjected to bending loads, are needed. So to be able to design a panel for axial loads no additional tests have to be performed. Only the usual tests according to EN 14509 are needed.

This report may only be reproduced in an unabridged version. A publication in extracts needs our written approval.

13 References

[1] D3.3 - part 4: Axially loaded sandwich panels. Deliverable of the EASIE project, June 2011.

[2] D3.2 - part 5: Tests on load application details of axially loaded sandwich panels. Deliverable of the EASIE project, September 2010.

[3] EN 14509:2006, Self-supporting double skin metal faced insulating panels –Factory made products –Specifications.

[4] European recommendations for sandwich panels. ECCS/CIB-Report – Publication 257, ECCS TWG 7.9 and CIB W056, 2000.

[5] EN 1990:2002: Eurocode – basis of structural design.

[6] EN 1993-1-1:2005, Eurocode 3: Design of steel structures – Part 1-1: General rules and rules for buildings.

[7] DIN 18800-2:2008: Stahlbauten – Teil 2: Stabilistätsfälle – Knicken von Stäben und Stabwerken (Steel structures – Part 2: Stability – Buckling of bars and sceletal structures).

[8] ETAG 21: Guideline for European technical approval of cold storage premises kits - Part 1: Cold Storage room kits and Part 2: Cold storage building envelope and building kits, EOTA 2005.

[9] Alber, D.: Das Knicken elastisch gebetteter Balken (Buckling of elastcally supported beams). Bauingenieur 82 (2007), S.95-102.

[10] Hetény, M.: Beams on elastic foundation. The University of Michigan Press, 1983.

[11] Izabel, D.: Formulaire de Résistance des Matériaux. Tome 4: Détermination des charges critiques de flambement d´éléments comprimés. Les Cahiers Pratiques du SNPPA, 2007.

[12] Linke, K.: Zum Tragverhalten von Profilsandwichplatten mit Stahldeckschichten und einem Polyurethan-Hartschaum-Kern bei kurz- und langzeitiger Belastung. Darmstadt,1978.

This report may only be reproduced in an unabridged version. A publication in extracts needs our written approval.

[13] Pfeiffer, L.: Durability Assessment of Sandwich Panel Construction. Institut für Sandwichtechnik – Mainz, 2005.

[14] Plantema, F.J.: Sandwich Construction - The Bending and Buckling of Sandwich Beams, Plates and Shells. New York: Wiley, 1966.

[15] Stamm, K., Witte, H.: Sandwichkonstruktionen – Berechnung, Fertigung, Ausführung. Springer – Verlag, 1974.

[16] Taras, A., Greiner, R.: Development of consistent buckling curves for torsional and lateral-torsional buckling. Steel Construction 1 (2008), S. 42-50.

This report may only be reproduced in an unabridged version. A publication in extracts needs our written approval.

Results of numerical investigations - wrinkling in mid-span

No.	t_F [mm]	$f_{y,F}$ [N/mm^2]	E_C [N/mm^2]	G_C [N/mm^2]	$\sigma_{cr,w}$ [N/mm^2]	λ_w	a_w [mm]	pre-defor-mation	σ_{ult} (FE) [N/mm^2]	reduction factor (FE)
1	0,5	150	24	12	322	0,683	21,05	a/150	159,7	1,064
2	0,5	150	16	8	246	0,781	24,09	a/150	135,2	0,901
3	0,5	200	14	7	225	0,943	25,19	a/150	138,9	0,694
4	0,5	200	8	4	155	1,137	30,36	a/150	103,5	0,517
5	0,5	200	6	3	128	1,251	33,41	a/150	90,4	0,452
6	0,5	360	8	4	155	1,525	30,36	a/150	125,2	0,348
7	0,5	240	4	2	97	1,569	38,25	a/150	75,8	0,316
8	0,5	360	6	3	128	1,679	33,41	a/150	105,7	0,294
9	0,5	360	4	2	97	1,922	38,25	a/150	83,2	0,231
10	0,5	400	4	2	97	2,026	38,25	a/150	84,9	0,212
11	0,5	360	2	1	61	2,421	48,19	a/150	54,6	0,152
12	0,5	150	24	12	322	0,683	21,05	a/200	160,8	1,072
13	0,5	150	16	8	246	0,781	24,09	a/200	138,1	0,921
14	0,5	200	14	7	225	0,943	25,19	a/200	145,6	0,728
15	0,5	200	8	4	155	1,137	30,36	a/200	111,3	0,557
16	0,5	200	6	3	128	1,251	33,41	a/200	95,2	0,476
17	0,5	360	8	4	155	1,525	30,36	a/200	130,3	0,362
18	0,5	240	4	2	97	1,569	38,25	a/200	79,3	0,330
19	0,5	360	6	3	128	1,679	33,41	a/200	109,7	0,305
20	0,5	360	4	2	97	1,922	38,25	a/200	85,7	0,238
21	0,5	400	4	2	97	2,026	38,25	a/200	79,3	0,198
22	0,5	360	2	1	61	2,421	48,19	a/200	56,3	0,156
23	0,5	280	6	3	128	1,481	33,41	a/200	103,8	0,371
24	0,4	280	6	3	128	1,481	26,73	a/200	104,7	0,374
25	0,75	280	6	3	128	1,481	50,12	a/200	102,6	0,366
26	0,5	280	4	2	97	1,695	38,25	a/200	82,0	0,293
27	0,4	280	4	2	97	1,695	30,60	a/200	82,4	0,294
28	0,75	280	4	2	97	1,695	57,37	a/200	81,3	0,290
29	0,5	280	8	4	155	1,345	30,36	a/200	122,6	0,438
30	0,4	280	8	4	155	1,345	24,29	a/200	123,7	0,442
31	0,75	280	8	4	155	1,345	45,54	a/200	121,3	0,433
32	0,5	360	6	3	128	1,679	33,41	a/200	109,73	0,305
33	0,4	360	6	3	128	1,679	26,73	a/200	110,2	0,306
34	0,75	360	6	3	128	1,679	50,12	a/200	108,3	0,301
35	0,5	360	4	2	97	1,922	38,25	a/200	85,7	0,238
36	0,4	360	4	2	97	1,922	30,60	a/200	86,6	0,241
37	0,75	360	4	2	97	1,922	57,37	a/200	84,8	0,236
38	0,5	360	8	4	155	1,525	30,36	a/200	130,3	0,362
39	0,4	360	8	4	155	1,525	24,29	a/200	131,5	0,365

This report may only be reproduced in an unabridged version. A publication in extracts needs our written approval.

No.	t_F [mm]	$f_{y,F}$ [N/mm²]	E_C [N/mm²]	G_C [N/mm²]	$\sigma_{cr,w}$ [N/mm²]	λ_w	a_w [mm]	pre-defor-mation	σ_{ult} (FE) [N/mm²]	reduction factor (FE)
40	0,75	360	8	4	155	1,525	45,54	a/200	128,9	0,358
41	0,5	200	6	3	128	1,251	33,41	a/200	95,2	0,476
42	0,4	200	6	3	128	1,251	26,73	a/200	96,1	0,481
43	0,75	200	6	3	128	1,251	50,12	a/200	94,4	0,472
44	0,5	200	4	2	97	1,432	38,25	a/200	75,9	0,380
45	0,4	200	4	2	97	1,432	30,60	a/200	76,4	0,382
46	0,75	200	4	2	97	1,432	57,37	a/200	75,4	0,377
47	0,5	200	8	4	155	1,137	30,36	a/200	111,3	0,557
48	0,4	200	8	4	155	1,137	24,29	a/200	110,4	0,552
49	0,75	200	8	4	155	1,137	45,54	a/200	109,3	0,547
50	0,5	150	24	12	322	0,683	21,05	a/250	162,1	1,081
51	0,5	150	16	8	246	0,781	24,09	a/250	141,0	0,940
52	0,5	200	14	7	225	0,943	25,19	a/250	150,4	0,752
53	0,5	200	8	4	155	1,137	30,36	a/250	115,5	0,577
54	0,5	200	6	3	128	1,251	33,41	a/250	98,7	0,493
55	0,5	360	8	4	155	1,525	30,36	a/250	134,1	0,372
56	0,5	240	4	2	97	1,569	38,25	a/250	81,5	0,340
57	0,5	360	6	3	128	1,679	33,41	a/250	111,7	0,310
58	0,5	360	4	2	97	1,922	38,25	a/250	88,2	0,245
59	0,5	400	4	2	97	2,026	38,25	a/250	89,7	0,224
60	0,5	360	2	1	61	2,421	48,19	a/250	57,4	0,160
61	0,5	150	24	12	322	0,683	21,05	a/500	167,2	1,114
62	0,5	150	16	8	246	0,781	24,09	a/500	149,5	0,997
63	0,5	200	14	7	225	0,943	25,19	a/500	165,7	0,829
64	0,5	200	8	4	155	1,137	30,36	a/500	126,8	0,634
65	0,5	200	6	3	128	1,251	33,41	a/500	104,1	0,521
66	0,5	360	8	4	155	1,525	30,36	a/500	143,3	0,398
67	0,5	240	4	2	97	1,569	38,25	a/500	88,6	0,369
68	0,5	360	6	3	128	1,679	33,41	a/500	117,8	0,327
69	0,5	360	4	2	97	1,922	38,25	a/500	93,0	0,258
70	0,5	400	4	2	97	2,026	38,25	a/500	94,1	0,235
71	0,5	360	2	1	61	2,421	48,19	a/500	59,7	0,166

This report may only be reproduced in an unabridged version. A publication in extracts needs our written approval.

Results of numerical investigations – crippling of the free edge

No.	t_F [mm]	$f_{y,F}$ [N/mm²]	E_C [N/mm²]	G_C [N/mm²]	$\sigma_{cr,c}$ [N/mm²]	λ_c	a_c [mm]	pre-defor-mation	σ_{ult} (FE) [N/mm²]	reduction factor (FE)
1	0,5	150	24	12	321,9	0,683	29,77	a/150	92,4	0,616
2	0,5	150	16	8	245,6	0,781	34,07	a/150	76,0	0,507
3	0,5	200	14	7	224,7	0,943	35,63	a/150	79,9	0,400
4	0,5	200	8	4	154,7	1,137	42,93	a/150	58,8	0,294
5	0,5	200	6	3	127,7	1,251	47,25	a/150	50,2	0,251
6	0,5	360	8	4	154,7	1,525	42,93	a/150	68,5	0,190
7	0,5	240	4	2	97,5	1,569	54,09	a/150	41,6	0,173
8	0,5	360	6	3	127,7	1,679	47,25	a/150	57,3	0,159
9	0,5	360	4	2	97,5	1,922	54,09	a/150	44,9	0,125
10	0,5	400	4	2	97,5	2,026	54,09	a/150	45,5	0,114
11	0,5	360	2	1	61,4	2,421	68,15	a/150	29,2	0,081
12	0,5	150	24	12	321,9	0,683	29,77	a/200	99,0	0,660
13	0,5	150	16	8	245,6	0,781	34,07	a/200	81,7	0,545
14	0,5	200	14	7	224,7	0,943	35,63	a/200	84,8	0,424
15	0,5	200	8	4	154,7	1,137	42,93	a/200	62,8	0,314
16	0,5	200	6	3	127,7	1,251	47,25	a/200	52,6	0,263
17	0,5	360	8	4	154,7	1,525	42,93	a/200	70,8	0,197
18	0,5	240	4	2	97,5	1,569	54,09	a/200	43,4	0,181
19	0,5	360	6	3	127,7	1,679	47,25	a/200	59,4	0,165
20	0,5	360	4	2	97,5	1,922	54,09	a/200	46,1	0,128
21	0,5	400	4	2	97,5	2,026	54,09	a/200	46,7	0,117
22	0,5	360	2	1	61,4	2,421	68,15	a/200	29,7	0,082
23	0,5	280	6	3	127,7	1,481	47,25	a/200	57,1	0,204
24	0,5	280	4	2	97,5	1,695	54,09	a/200	44,5	0,159
25	0,5	280	8	4	154,7	1,345	42,93	a/200	67,9	0,243
26	0,5	150	24	12	321,9	0,683	29,77	a/250	103,9	0,693
27	0,5	150	16	8	245,6	0,781	34,07	a/250	85,8	0,572
28	0,5	200	14	7	224,7	0,943	35,63	a/250	89,2	0,446
29	0,5	200	8	4	154,7	1,137	42,93	a/250	65,3	0,327
30	0,5	200	6	3	127,7	1,251	47,25	a/250	55,0	0,275
31	0,5	360	8	4	154,7	1,525	42,93	a/250	72,2	0,200
32	0,5	240	4	2	97,5	1,569	54,09	a/250	44,6	0,186
33	0,5	360	6	3	127,7	1,679	47,25	a/250	60,6	0,168
34	0,5	360	4	2	97,5	1,922	54,09	a/250	47,0	0,130
35	0,5	400	4	2	97,5	2,026	54,09	a/250	47,5	0,119
36	0,5	360	2	1	61,4	2,421	68,15	a/250	30,2	0,084

This report may only be reproduced in an unabridged version. A publication in extracts needs our written approval.

No.	t_F [mm]	$f_{y,F}$ [N/mm²]	E_C [N/mm²]	G_C [N/mm²]	$\sigma_{cr,c}$ [N/mm²]	λ_c	a_c [mm]	pre-defor-mation	σ_{ult} (FE) [N/mm²]	reduction factor (FE)
37	0,5	150	24	12	321,9	0,683	29,77	a/500	119,0	0,794
38	0,5	150	16	8	245,6	0,781	34,07	a/500	99,0	0,660
39	0,5	200	14	7	224,7	0,943	35,63	a/500	99,5	0,498
40	0,5	200	8	4	154,7	1,137	42,93	a/500	70,9	0,354
41	0,5	200	6	3	127,7	1,251	47,25	a/500	59,5	0,298
42	0,5	360	8	4	154,7	1,525	42,93	a/500	76,3	0,212
43	0,5	240	4	2	97,5	1,569	54,09	a/500	47,2	0,197
44	0,5	360	6	3	127,7	1,679	47,25	a/500	63,2	0,176
45	0,5	360	4	2	97,5	1,922	54,09	a/500	48,7	0,135
46	0,5	400	4	2	97,5	2,026	54,09	a/500	49,1	0,123
47	0,5	360	2	1	61,4	2,421	68,15	a/500	31,1	0,086

This report may only be reproduced in an unabridged version. A publication in extracts needs our written approval.

Slenderness of faces of panels used for the tests – wrinkling in mid-span

type of panel	E_C [N/mm²]	G_C [N/mm²]	$f_{y,F}$ [N/mm²]	EI_F [Nmm²/mm]	A_F [mm²/mm]	$\sigma_{cr,w}$ 1) [N/mm²]	λ_w 2)
A	3,10	2,93	358	17635	0,474	208,2	1,311
B	5,08	3,56	403	29242	0,762	192,8	1,446
C	8,47	4,18	409	3028	0,540	159,9	1,600
E	10,71	9,82	467	4477	0,475	297,6	1,253

1) elastic buckling load for wrinkling of face in mid-span

$$\sigma_{cr,w} = \frac{3}{A_F} \cdot \sqrt[3]{\frac{2}{9} \cdot EI_F \cdot G_C \cdot E_C}$$

2) slenderness of face (wrinkling in mid-span)

$$\lambda_w = \sqrt{\frac{f_{y,F}}{\sigma_{cr,w}}}$$

Imperfection factor α of panels used for the tests

type of panel	wrinkling stress σ_w (mean values) [N/mm²]	$f_{y,F}$ [N/mm²]	reduction factor 3)	slenderness λ_w of the face 2)	imperfection factor α 4)
A	201	358	0,561	1,311	≤ 0,21
B	201	403	0,499	1,446	≤ 0,21
C	176	409	0,430	1,600	≤ 0,21
E	196	467	0,281	1,253	2,60

3) reduction factor for wrinkling

$$\chi_w = \frac{\sigma_w}{f_{y,F}}$$

4) imperfection factor

$$\alpha = \frac{1 + \chi_w \cdot \lambda_w^2 \cdot (\chi_w - 1) - \chi}{\chi_w \cdot (\lambda_w - \lambda_0)} \geq 0{,}21$$

This report may only be reproduced in an unabridged version. A publication in extracts needs our written approval.

Slenderness of faces of panels used for the tests – crippling of a free edge

type of panel	E_C [N/mm²]	G_C [N/mm²]	$f_{y,F}$ [N/mm²]	EI_F [Nmm²/mm]	A_F [mm²/mm]	$\sigma_{cr,c}$ [5] [N/mm²]	λ_c [6]
A	3,10	2,93	358	17635	0,474	104,1	1,854
B	5,08	3,56	403	29242	0,762	96,4	2,044
C	8,47	4,18	409	3028	0,540	79,9	2,262
E	10,71	9,82	467	4477	0,475	148,8	1,772

[5] elastic buckling load for crippling of a free edge

$$\sigma_{cr,c} = \frac{3}{2 \cdot A_F} \cdot \sqrt[3]{\frac{2}{9} \cdot EI_F \cdot G_C \cdot E_C}$$

[6] slenderness of face (crippling of a free edge)

$$\lambda_c = \sqrt{\frac{f_{y,F}}{\sigma_{cr,c}}}$$

Crippling stress σ_c* of panels used for the tests

type of panel	yield strength [N/mm²]	imperfection factor α [4]	slenderness λ_c of the face [6]	reduction factor for crippling [7]	crippling stress σ_c* [8] [N/mm²]
A	358	0,21	1,854	0,265	95,0
B	403	0,21	2,044	0,220	88,7
C	409	0,21	2,262	0,181	74,1
E	467	2,60	1,772	0,155	72,6

[7] reduction factor for crippling of free edge

$$\chi_c = \frac{1}{\phi + \sqrt{\phi^2 - \lambda_c^2}} \leq 1$$

$$\phi = \frac{1}{2} \cdot \left(1 + \alpha \cdot (\lambda_c - \lambda_0) + \lambda_c^2\right); \quad \lambda_0 = 0{,}7$$

[8] crippling stress σ_c*

$$\sigma_c^* = \chi_c \cdot f_{y,F}$$

This report may only be reproduced in an unabridged version. A publication in extracts needs our written approval.